REPORT 1181

STRUCTURAL RESPONSE TO DISCRETE AND CONTINUOUS GUSTS OF AN AIRPLANE HAVING WING-BENDING FLEXIBILITY AND A CORRELATION OF CALCULATED AND FLIGHT RESULTS

By JOHN C. HOUBOLT and ELDON E. KORDES

Langley Aeronautical Laboratory
Langley Field, Va.

National Advisory Committee for Aeronautics

Headquarters, 1512 H Street NW., Washington 25, D. C.

Created by act of Congress approved March 3, 1915, for the supervision and direction of the scientific study of the problems of flight (U. S. Code, title 50, sec. 151). Its membership was increased from 12 to 15 by act approved March 2, 1929, and to 17 by act approved May 25, 1948. The members are appointed by the President, and serve as such without compensation.

Conduct, under unified control, for all agencies, of scientific research on the fundamental problems of flight

REPORT 1181

STRUCTURAL RESPONSE TO DISCRETE AND CONTINUOUS GUSTS OF AN AIRPLANE HAVING WING BENDING FLEXIBILITY AND A CORRELATION OF CALCULATED AND FLIGHT RESULTS[1]

By John C. Houbolt and Eldon E. Kordes

SUMMARY

An analysis is made of the structural response to gusts of an airplane having the degrees of freedom of vertical motion and wing bending flexibility and basic parameters are established. A convenient and accurate numerical solution of the response equations is developed for the case of discrete-gust encounter, an exact solution is made for the simpler case of continuous-sinusoidal-gust encounter, and the procedure is outlined for treating the more realistic condition of continuous random atmospheric turbulence, based on the methods of generalized harmonic analysis.

Correlation studies between flight and calculated results are then given to evaluate the influence of wing bending flexibility on the structural response to gusts of two twin-engine transports and one four-engine bomber. It is shown that calculated results obtained by means of a discrete-gust approach reveal the general nature of the flexibility effects and lead to qualitative correlation with flight results. In contrast, calculations by means of the continuous-turbulence approach show good quantitative correlation with flight results and indicate a much greater degree of resolution of the flexibility effects.

INTRODUCTION

In the design of aircraft the condition of gust encounter has become critical in more and more instances, mainly because of increased flight speeds and because of configuration changes. Aircraft designers have therefore placed greater emphasis on obtaining more nearly applicable methods for predicting the stresses that develop. As a result, the number of papers on this subject has significantly increased. (See, for example, refs. 1 to 16.) Many of the papers have treated the airplane as a rigid body and in so doing have dealt with either the degree of freedom of vertical motion alone (refs. 1 to 4) or with the degrees of freedom of vertical motion and pitch (refs. 3, 5, and 6). In the main, these rigid-body treatments tacitly involve the concept of "discrete," "isolated" gusts, but more recently steps have been taken to treat the more realistic condition of continuous-turbulence encounter in an explicit manner (see refs. 6 to 9).

In addition to rigid-body effects, one of the more important items that has been of concern in the consideration of gust penetration is the influence that wing flexibility has on structural response. This concern has two main aspects: (1) that including wing flexibility may lead to the calculation of higher stresses than would be obtained by rigid-body treatment of the problem and (2) that wing flexibility may introduce some error when an airplane is used as an instrument for measuring gust intensity. Thus, several papers have also appeared which treat the airplane as a flexible body. In most of these papers the approach used involves the development of the structural response in terms of the natural modes of vibration of the airplane (refs. 10 to 15). In others the approach is more unusual, as, for example, reference 16 which deals with the simultaneous treatment of the conditions of equilibrium between aerodynamic forces and structural deformation at a number of points along the wing span. Whatever the approach, however, these flexible-body analyses have two main shortcomings. They too have adhered to the concept of simple-gust or discrete-gust encounter (ref. 10 is an exception) and also they are not very well suited for making trend studies without excessive computation time.

The intent of the present report is to shed further light upon the case of gust penetration of an airplane having the degrees of freedom of vertical motion and wing bending. It has several objectives: (1) to establish some of the basic parameters that are involved when wing bending flexibility is included, (2) to develop a method of solution which is fairly well suited for trend studies without excessive computation time, (3) to evolve methods for treating continuous turbulence as well as discrete gusts, and (4) to show the degree of correlation that can be obtained between flight-test and analytical results and, through this correlation, to assess how well flexibility effects may be analyzed. In effect, this report is a composite of the discrete-gust studies made jointly by the authors in references 11 and 12 and of the continuous-turbulence studies made by the first author in reference 10 and in unpublished form.

The report is developed as follows: The equations for response (including accelerations, displacements, and bending moments) are derived and the basic parameters outlined. A simple solution of these equations follows for both discrete-gust encounter and for continuous-sinusoidal-gust encounter. Next, the procedure for treating continuous atmospheric turbulence is outlined. Then, the correlation studies involving a comparison of flight-test results with the calculated results obtained for both discrete-gust and continuous-turbulence conditions are given.

[1] Supersedes NACA TN 3006 by John C. Houbolt, 1953, also contains essential material from NACA TN 2763 by John C. Houbolt and Eldon E. Kordes, 1952, and NACA TN 2797 by Eldon E. Kordes and John C. Houbolt, 1953.

SYMBOLS

a	slope of lift curve
a_n	deflection coefficient for nth mode, function of time alone
A	aspect ratio of wing
b	span of wing
c	chord of wing
c_0	chord of wing midspan
d, e, h	see equation (23b)
E	Young's modulus of elasticity
$f(s)$	nondimensional gust force, $\int_0^s \frac{u'}{U}\psi(s-\sigma)d\sigma$
F	external applied load per unit span
g	acceleration due to gravity
H	distance to gust peak, chords
I	bending moment of inertia
k	reduced frequency, $\frac{\omega c_0}{2V}$
K_j	nondimensional bending-moment factor $\left(M_j=K_j\frac{a}{2}\rho VUM_{c_0}\right)$
L	wave length
L_g	aerodynamic lift per unit span of wing due to gust
L_v	aerodynamic lift per unit span of wing due to vertical motion of airplane
m	mass per unit span of wing
M_j	net incremental bending moment at wing station j
$M_{c_n}=\int_{y_j}^{b/2} cw_n(y-y_j)dy$	
$M_{m_n}=\int_{y_j}^{b/2} mw_n(y-y_j)dy$	
M_n	generalized mass of nth mode
Δ_n	incremental number of g acceleration
N_p	see equation (58a)
p	load intensity per unit spanwise length
r_1, r_2, r_3	see equations (18), (24), and (13)
s	distance traveled, $\frac{2V}{c_0}t$, half-chords
S	wing area
t, τ	time
$T(\omega)$, $T(\Omega)$	frequency-response function
u	vertical velocity of gust or random disturbance
U	maximum vertical velocity of gust
V	forward velocity of flight
W	total weight of airplane
w	deflection of elastic axis of wing, positive upward
w_n	deflection of elastic axis in nth mode, given in terms of unit tip deflection
y	distance along wing measured from airplane center line
z_n	response coefficient based on a_n, $\frac{V}{Uc_0}a_n$
α	second derivative of z_0 with respect to s
β	second derivative of z_1 with respect to s
δ	absolute value of center-line deflection of fundamental mode in terms of unit tip displacement
ϵ	distance interval, half-chords; also, strain
η_n	nondimensional bending-moment parameter, $\frac{8M_{m_n}}{a\rho c_0 M_{c_0}}$
$\theta=1-\phi$	
λ	reduced-frequency parameter, $\frac{\omega_1 c_0}{2V}$
μ_n	nondimensional relative-density parameter, $\frac{8M_n}{a\rho c_0 S}$
ρ	mass density of air
σ	standard deviation; also, distance traveled, $\frac{2V}{c_0}\tau$, half-chords
$1-\phi$	function which denotes growth of lift on an airfoil following a sudden change in angle of attack (Wagner function)
$\Phi(\omega)$, $\Phi(\Omega)$	power-spectral-density functions
ψ	function which denotes growth of lift on rigid wing entering a sharp-edge gust (Küssner function)
ω	circular frequency
ω_n	natural circular frequency of vibration of nth mode
Ω	frequency, $\Omega=\frac{2\pi}{L}=\frac{\omega}{V}=\frac{2k}{c_0}$

Subscripts:

exp	experimental
f	flexible
F	fuselage
i	input
j	spanwise station
m	number of distance intervals traveled
n	natural modes of vibration
N	nodal
o	output
r	rigid
theo	theoretical

Notation:

| |	column matrix when used in matrix equations
[ ]	square matrix

Dots are used to denote derivatives with respect to time; primes denote derivatives with respect to s or σ; a bar above a quantity denotes the time average; and vertical bars about a quantity denote the modulus.

ANALYSIS OF RESPONSE TO ARBITRARY GUSTS

EQUATIONS FOR STRUCTURAL RESPONSE

The following analysis treats the problem of determining the stresses that develop in an airplane flying through vertical gusts on the assumption that the airplane is free to respond only in vertical motion and wing bending. The case of the transient response to arbitrary gusts is considered first. A subsequent section is then devoted to the case of random disturbances in which explicit consideration is given the continuous nature of atmospheric turbulence.

Equations of motion.—It is convenient to treat the problem simply as one of determining the elastic and translational response of a free-free elastic beam subject to arbitrary dynamic forces. For dynamic forces of intensity F per unit length, the differential equation for wing bending is, if structural damping is neglected,

$$\frac{\partial^2}{\partial y^2} EI \frac{\partial^2 w}{\partial y^2} = -m\ddot{w} + F \tag{1}$$

where w is the deflection of the elastic axis referred to a fixed reference plane. The task of determining the deflection that results from the applied forces F may be handled conveniently by expressing the deflection in terms of the natural free-free vibrational modes of the wing.

The wing deflection is thus assumed to be given by the equation

$$w = a_0 w_0 + a_1 w_1 + a_2 w_2 + \ . \ . \ . \tag{2}$$

where the a_n's are functions of time alone, and the w_n's represent the deflections of the various modes along the elastic axis of the wing, each being given in terms of a unit tip deflection. In equation (2), w_0 represents the rigid-body mode and has a constant unit displacement over the span; the other w's are elastic-body modes which satisfy the differential equation

$$\frac{\partial^2}{\partial y^2} EI \frac{\partial^2 w_n}{\partial y^2} = \omega_n^2 m w_n \tag{3}$$

and the orthogonality condition

$$\int_{-b/2}^{b/2} m w_m w_n \, dy = 0 \qquad (m \neq n) \tag{4}$$

$$= M_n \qquad (m = n) \tag{5}$$

In accordance with the Galerkin procedure for solving differential equations, equation (2) is first substituted into equation (1) to give, after use is made of equation (3),

$$a_1 \omega_1^2 m w_1 + a_2 \omega_2^2 m w_2 + \ . \ . \ . \ = -m(\ddot{a}_0 w_0 + \ddot{a}_1 w_1 + \ . \ . \ .) + F \tag{6}$$

Now if this equation is multiplied through by w_n, then is integrated over the wing span, and use is made of equations (4) and (5), the following basic equation results:

$$M_n \ddot{a}_n + \omega_n^2 M_n a_n = \int_{-b/2}^{b/2} F w_n \, dy \tag{7}$$

which allows for the solution of the coefficients a_n if the applied forces F are known. This equation applies for the translational mode $n=0$, for which case $\omega_0 = 0$, as well as for all the elastic-body modes. The quantity M_n appearing in the equation is commonly called the generalized mass of the nth mode.

For the present case of the airplane flying through a gust, the force F is composed of two parts: a part designated by L_v due to the vertical motion of the airplane (including both rigid-body and bending displacements) and a part L_g resulting directly from the gust (this latter part is the gust force which would develop on the wing considered rigid and restrained against vertical motion). On the basis of a strip type of analysis, these two parts are defined as follows:

$$F = L_v + L_g = -\frac{a}{2} \rho c V \int_0^t \ddot{w} \, [1 - \phi \, (t-\tau)] d\tau + \frac{a}{2} \rho c V \int_0^t \dot{u} \psi (t-\tau) d\tau \tag{8}$$

where $t=0$ is taken at the beginning of gust penetration. $1-\phi(t)$ is a function (commonly referred to as the Wagner function) which denotes the growth of lift on a wing following a sudden change in angle of attack and for two-dimensional incompressible flow is given by the approximation

$$[1 - \phi \, (t)]_{A=\infty} = 1 - 0.165 e^{-0.09 \frac{V}{c} t} - 0.335 e^{-0.6 \frac{V}{c} t} \tag{9}$$

and $\psi(t)$ is a function (commonly referred to as the Küssner function) which denotes the growth of lift on a rigid wing penetrating a sharp-edge gust and for two-dimensional incompressible flow is given by the approximation

$$[\psi \, (t)]_{A=\infty} = 1 - 0.5 e^{-0.26 \frac{V}{c} t} - 0.5 e^{-2 \frac{V}{c} t} \tag{10}$$

Figure 1 is a plot of equations (9) and (10).

An additional term which involves the apparent air mass should be included in equation (8); this mass term is inertial in character and may be included with the structural mass (see ref. 16) although it is usually small in comparison. The lift-curve slope a may be chosen so as to include approximate overall corrections for aspect ratio and compressibility effects.

The remainder of the analysis is restricted to uniform spanwise gusts and the assumption is made that the response will be given with sufficient accuracy by considering only two degrees of freedom: vertical motion and fundamental wing bending. On this basis, if w as given by the first two terms in equation (2) is substituted into equation (8) and the resulting equation for F is substituted into equation (7), the following two response equations result when n is set

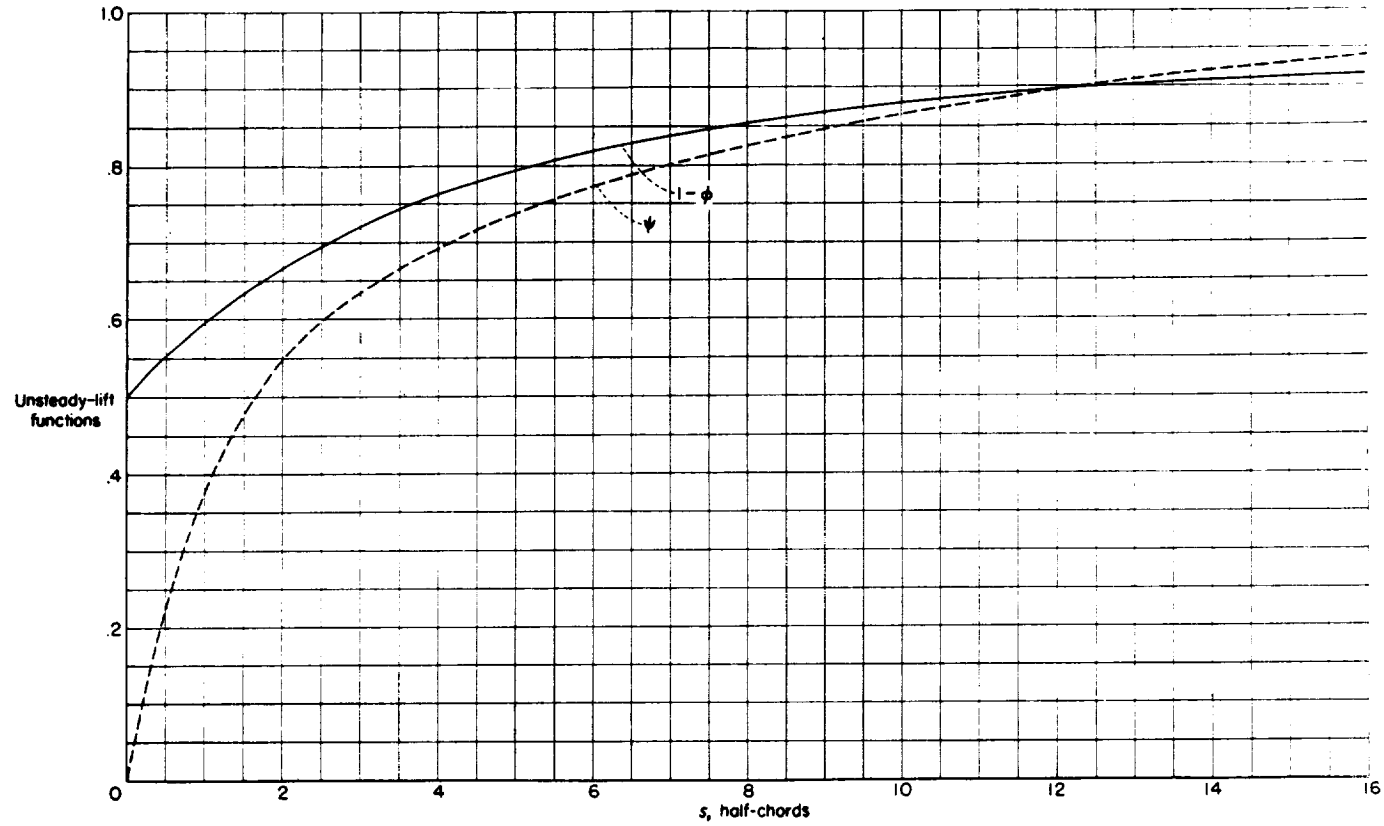

FIGURE 1.—Unsteady-lift functions (see eqs. (9) and (10)) where, for a sharp-edge gust, the gust force $f(s)=\psi(s)$.

equal to 0 and 1, respectively:

$$\frac{2M_0}{a\rho V S}\ddot{a}_0=-\int_0^t\left(\ddot{a}_0+\frac{S_1}{S}\ddot{a}_1\right)[1-\phi(t-\tau)]\,d\tau+\int_0^t\dot{u}\psi(t-\tau)\,d\tau \tag{11}$$

and

$$\frac{2M_1}{a\rho V S}\ddot{a}_1+\frac{\omega_1^2 2M_1}{a\rho V S}a_1=-\int_0^t\left(\frac{S_1}{S}\ddot{a}_0+\frac{S_2}{S}\ddot{a}_1\right)[1-\phi(t-\tau)]\,d\tau+\frac{S_1}{S}\int_0^t\dot{u}\psi(t-\tau)\,d\tau \tag{12}$$

where (because of mode symmetry)

$$\left.\begin{aligned}S&=2\int_0^{b/2}c\,dy\\S_1&=2\int_0^{b/2}cw_1\,dy\\S_2&=2\int_0^{b/2}cw_1^2dy\end{aligned}\right\} \tag{13}$$

Equations (11) and (12) may be put in convenient nondimensional form by introducing the notation

$$s=\frac{2V}{c_0}t \tag{14a}$$

or

$$\sigma=\frac{2V}{c_0}\tau \tag{14b}$$

and

$$z_n=\frac{V}{l}a_n \tag{15}$$

where c_0 is the midspan chord of the wing and V is the maximum vertical velocity of the gust. With this notation, equations (11) and (12) may be written

$$\mu_0 z_0''=-2\int_0^s(z_0''+r_1z_1'')[1-\phi(s-\sigma)]d\sigma+\int_0^s\frac{u'}{l}\psi(s-\sigma)d\sigma \tag{16}$$

and

$$\mu_1 z_1''+\mu_1\lambda^2 z_1=-2\int_0^s(r_1z_0''+r_2z_1'')[1-\phi(s-\sigma)]d\sigma+r_1\int_0^s\frac{u'}{l}\psi(s-\sigma)d\sigma \tag{17}$$

where

$$\left.\begin{aligned}\mu_0&=\frac{8M_0}{a\rho c_0 S}\\\mu_1&=\frac{8M_1}{a\rho c_0 S}\\\lambda&=\frac{\omega_1 c_0}{2V}\\r_1&=\frac{S_1}{S}\\r_2&=\frac{S_2}{S}\end{aligned}\right\} \tag{18}$$

and a prime denotes a derivative with respect to σ. Equations (16) and (17) are the basic response equations in the present analysis. The five parameters appearing in these equations and given by equations (18) depend upon the forward velocity, air density, lift-curve slope, and the air-

plane physical characteristics: the wing plan form, wing bending stiffness, and wing mass distribution. Experience has shown that variations in the physical characteristics cause significant variations in the first three of the five parameters, while the last two vary only to a minor extent. The first three are therefore the most basic parameters; μ_0 is a relative-density factor, frequently referred to as a mass parameter, and is associated with vertical free-body motion of the airplane; μ_1, similar to μ_0, is the mass parameter associated with the fundamental mode; and λ, by its nature, may be interpreted as a reduced-frequency parameter similar to that used in flutter analysis.

It is significant to note that, if any one of the three quantities z_0, z_1, and u appearing in equations (16) and (17) is specified or known, the other two may be determined. Thus, if the gust is known, the response may be determined or, conversely, if either z_0 or z_1 is known; the gust may be determined. A useful equation relating z_0 and z_1 may be found by combining equations (16) and (17) so as to eliminate the integral dealing with the gust. The result is the equation

$$\frac{\mu_1}{r_1}(z_1''+\lambda^2 z_1)+2\left(\frac{r_2}{r_1}-r_1\right)\int_0^s z_1''[1-\phi(s-\sigma)]d\sigma=\mu_0 z_0'' \qquad (19)$$

which is used subsequently.

It may also be of interest to note that $\mu_0 z_0''$, in effect, defines a frequently used acceleration ratio. From equations (15) and (14), the rigid-body component of the vertical acceleration may be written

$$\ddot{a}_0=\frac{4VU}{c_0}z_0''$$

or, when expressed in terms of the incremental number of g's,

$$\Delta n=\frac{\ddot{a}_0}{g}=\frac{4VU}{c_0 g}z_0''$$

An acceleration factor Δn_s based on quasi-steady flow and peak gust velocity is now introduced according to the definition

$$\Delta n_s W=\frac{a}{2}\rho S V^2\frac{U}{V}$$

The ratio $\frac{\Delta n}{\Delta n_s}$ is thus found to be

$$\frac{\Delta n}{\Delta n_s}=\mu_0 z_0''$$

Where the gust shape is represented analytically and the unsteady-lift functions are taken in the form given by equations (9) and (10), solution of the response equations may be made by the Laplace transform method, but such a solution is more laborious than desired. Therefore, a numerical procedure which permits a rather rapid solution of the equations has been devised for the case of discrete-gust encounter and is presented in a subsequent section. It may be well to mention, however, that the response equations are suitable for solution by some of the analog computing machines.

Bending stresses.—The bending moment and, hence, the bending stresses that develop in the wing due to the gust may be found as follows: The right-hand side of equation (1) defines the loading on the wing; suppose that this loading is denoted by p, then

$$p=-m\ddot{w}+F$$

By use of equations (2) and (8) and the notation of equations (14) and (15), this equation becomes

$$p=-m\frac{4VU}{c_0}(z_0''+z_1''w_1)-a\rho cVU\int_0^s(z_0''+z_1''w_1)[1-\phi(s-\sigma)]d\sigma+\frac{a}{2}\rho cV\int_0^s u'\psi(s-\sigma)d\sigma$$

where, as before, only the first two deflection terms have been retained. If the moment of this loading is taken about a given wing station, say y_j, the following equation for incremental bending moment at that station will result:

$$M_j=\int_{y_j}^{b/2}p(y-y_j)dy$$

$$=-\frac{4VU}{c_0}(M_{m_0}z_0''+M_{m_1}z_1'')-a\rho VU\int_0^s(M_{c_0}z_0''+M_{c_1}z_1'')[1-\phi(s-\sigma)]d\sigma+\frac{a}{2}\rho VM_{c_0}\int_0^s u'\psi(s-\sigma)d\sigma \qquad (20)$$

where the M's bearing double subscripts are first moments defined as follows:

$$\left.\begin{aligned}M_{m_0}&=\int_{y_j}^{b/2}m(y-y_j)dy & M_{c_0}&=\int_{y_j}^{b/2}c(y-y_j)dy\\ M_{m_1}&=\int_{y_j}^{b/2}mw_1(y-y_j)dy & M_{c_1}&=\int_{y_j}^{b/2}cw_1(y-y_j)dy\end{aligned}\right\} \qquad (21)$$

and y_j is the station being considered. Dividing equation (20) by the quantity $\frac{a}{2}\rho VUM_{c_0}$ gives the following equation which is considered to define a bending-moment factor K_j at wing station y_j

$$K_j=\frac{M_j}{\frac{a}{2}\rho VUM_{c_0}}=-\frac{8M_{m_0}}{a\rho c_0 M_{c_0}}\left(z_0''+\frac{M_{m_1}}{M_{m_0}}z_1''\right)-2\int_0^s\left(z_0''+\frac{M_{c_1}}{M_{c_0}}z_1''\right)[1-\phi(s-\sigma)]d\sigma+\int_0^s\frac{u'}{U}\psi(s-\sigma)d\sigma \qquad (22)$$

The factor $\frac{a}{2}\rho VUM_{c_0}$ may be regarded as the maximum aerodynamic bending moment that would be developed by the gust under conditions of quasi-steady flow and with the wing considered rigid and restrained against vertical motion at the root. The bending-moment factor K_j may thus be seen to be the ratio of the actual dynamic bending moment that occurs to this quasi-steady bending moment and therefore may be regarded as a response or an alleviation factor.

A more convenient form for the bending-moment factor may be obtained by solving equations (16) and (17) simultaneously for the quantities $\int_0^s z_0''[1-\phi(s-\sigma)]d\sigma$ and

$\int_0^s z_1''[1-\phi(s-\sigma)]d\sigma$ and substituting these values into equation (22). With these operations the following equation results:

$$K_j=\frac{M_j}{\frac{a}{2}\rho VUM_{c_0}}$$
$$=dz_0''+ez_1''+h\lambda^2 z_1 \tag{23a}$$

where

$$\left.\begin{aligned} d&=\frac{r_3r_1-r_2}{r_1^2-r_2}\mu_0-\eta_0\\ e&=\frac{r_1-r_3}{r_1^2-r_2}\mu_1-\eta_1\\ h&=\frac{r_1-r_3}{r_1^2-r_2}\mu_1 \end{aligned}\right\} \tag{23b}$$

and

$$\left.\begin{aligned} r_3&=\frac{M_{c_1}}{M_{c_0}}\\ \eta_0&=\frac{8M_{m_0}}{a\rho c_0M_{c_0}}\\ \eta_1&=\frac{8M_{m_1}}{a\rho c_0M_{c_0}} \end{aligned}\right\} \tag{24}$$

It is seen that, when bending moments are being determined, three additional basic parameters (eqs. (24)) appear. The similarity of η_0 and η_1 to μ_0 and μ_1 is to be noted; first moments of masses and areas are involved rather than masses and areas.

Reduction to rigid case.—It may be of interest to show the reduction of the response equation to the case of the airplane considered as a rigid body. Thus, if z_1 is equated to zero in equation (16), the following equation for rigid-body response is obtained:

$$\mu_0 z_{0_r}''=-2\int_0^s z_{0_r}''[1-\phi(s-\sigma)]d\sigma+\int_0^s\frac{u'}{U}\psi(s-\sigma)d\sigma \tag{25}$$

If z_1'' is set equal to zero in equation (22) and use is made of equation (25), the following equation for the bending-moment parameter for the rigid-body case is obtained

$$K_{j_r}=(\mu_0-\eta_0)z_{0_r}'' \tag{26}$$

where z_{0_r}'' is the nondimensional acceleration of the airplane considered as a rigid body.

SOLUTION OF RESPONSE EQUATIONS

The case of discrete-gust encounter.—In this section a rather simple numerical solution of the response equations (16) and (17) is presented for the case where discrete gusts are suddenly encountered. The procedure is readily adapted to either manual or punch-card-machine calculations.

The derivation proceeds on the basis that the response due to a given gust is to be determined. The airplane, just before gust penetration, is considered to be in level flight and, hence, has the initial conditions that the vertical displacement and vertical velocity are both zero. These conditions mean that z_0, z_1, z_0', and z_1' are all zero at $s=0$. The gust force can be shown to start from zero and, therefore, the additional initial conditions can be established that z_0'' and z_1'' are also zero at $s=0$. By the numerical procedure, solution for the response at successive values of s of increment ϵ will be made and, for the case being considered, it is found advantageous to solve directly for the accelerations rather than the displacements.

In order to make the presentation more compact, the following notation is introduced:

$$\left.\begin{aligned} \alpha&=z_0''\\ \beta&=z_1''\\ \theta&=1-\phi \end{aligned}\right\} \tag{27a}$$

and

$$f(s)=\int_0^s\frac{u'}{U}\psi(s-\sigma)\,d\sigma \tag{27b}$$

With this notation, equation (16) would appear simply as

$$\mu_0\alpha=-2\int_0^s(\alpha+r_1\beta)\theta(s-\sigma)\,d\sigma+f(s) \tag{28}$$

In accordance with numerical-evaluation procedures, the interval between 0 and s is divided into m equal stations of interval ϵ so that $s=m\epsilon$. The product of $(\alpha+r_1\beta)$ and $\theta(s-\sigma)$ is assumed formed at each station and, with the use of the trapezoidal method for determining areas, the unsteady-lift integral in equation (28) may be written in terms of values of α and β at successive stations as follows, where the mth station corresponds to the value s:

$$\int_0^s(\alpha+r_1\beta)\theta(s-\sigma)d\sigma=\epsilon\left(\theta_{m-1}\alpha_1+\theta_{m-2}\alpha_2+\ \ldots\ +\theta_1\alpha_{m-1}+\frac{1}{2}\theta_0\alpha_m\right)+\epsilon r_1\left(\theta_{m-1}\beta_1+\theta_{m-2}\beta_2+\ \ldots\ +\theta_1\beta_{m-1}+\frac{1}{2}\theta_0\beta_m\right) \tag{29}$$

in which θ_0, θ_1, . . . are, respectively, the values of the $1-\phi$ function at $s=0$, $s=\epsilon$, . . . (α_0 and β_0 do not appear because of the initial conditions). With this equation, equation (28) may be written at various values of s or at successive values of m; the result, for example, for $m=1$ is

$$\mu_0\alpha_1=-\epsilon\theta_0\alpha_1-\epsilon r_1\theta_0\beta_1+f_1$$

and for $m=2$,

$$\mu_0\alpha_2=-\epsilon(2\theta_1\alpha_1+\theta_0\alpha_2)-\epsilon r_1(2\theta_1\beta_1+\theta_0\beta_2)+f_2$$

where f_1 and f_2 are the values of the gust-force integral at $s=\epsilon$ and $s=2\epsilon$.

The equations thus formed may be combined in the following matrix equation:

$$\begin{bmatrix} \mu_0+\theta_0\epsilon & & & & \\ 2\theta_1\epsilon & \mu_0+\theta_0\epsilon & & & \\ 2\theta_2\epsilon & 2\theta_1\epsilon & \mu_0+\theta_o\epsilon & & \\ \cdot & \cdot & \cdot & & \\ \cdot & \cdot & \cdot & & \\ \cdot & \cdot & \cdot & & \\ 2\theta_{m-1}\epsilon & 2\theta_{m-2}\epsilon & \cdot\ \cdot\ \cdot & & \mu_0+\theta_0\epsilon \end{bmatrix} \begin{vmatrix} \alpha_1 \\ \alpha_2 \\ \alpha_3 \\ \cdot \\ \cdot \\ \cdot \\ \alpha_m \end{vmatrix} + \begin{bmatrix} r_1\theta_0\epsilon & & & & \\ 2r_1\theta_1\epsilon & r_1\theta_0\epsilon & & & \\ 2r_1\theta_2\epsilon & 2r_1\theta_1\epsilon & r_1\theta_0\epsilon & & \\ \cdot & \cdot & \cdot & & \\ \cdot & \cdot & \cdot & & \\ \cdot & \cdot & \cdot & & \\ 2r_1\theta_{m-1}\epsilon & 2r_1\theta_{m-2}\epsilon & \cdot\ \cdot\ \cdot & & r_1\theta_0\epsilon \end{bmatrix} \begin{vmatrix} \beta_1 \\ \beta_2 \\ \beta_3 \\ \cdot \\ \cdot \\ \cdot \\ \beta_m \end{vmatrix} = \begin{vmatrix} f_1 \\ f_2 \\ f_3 \\ \cdot \\ \cdot \\ \cdot \\ f_m \end{vmatrix} \tag{30a}$$

which may be abbreviated

$$[A]|\alpha|+[B]|\beta|=|f| \tag{30b}$$

The simplicity of the matrices A and B, and all square matrices to follow, is to be noted; the matrices are triangular and all elements in one column are merely the elements in the previous column moved down one row. Thus, only the elements in the first columns have to be known to define completely the matrices.

Now instead of considering directly the second response equation, equation (17), it is expedient to consider equation (19). According to the derivation presented in appendix A, the value of z_1 at $s=m\epsilon$ may be approximated in terms of the past-history value of z_1'' by the following equation:

$$z_{1_m}=\epsilon^2\left[(m-1)\beta_1+\ \cdot\ \cdot\ \cdot\ +2\beta_{m-2}+\beta_{m-1}+\frac{1}{6}\beta_m\right] \tag{31}$$

where β_1, β_2, . . . are the values of z_1'' at $s=\epsilon$, $s=2\epsilon$, ... If this equation is used to replace z_1 in equation (19) and the unsteady-lift integral is manipulated similarly to the integral in equation (28), equations are obtained for successive values of m which involve only the unknowns α and β. The results may be combined in the following matrix equation:

$$\begin{bmatrix} \frac{\mu_1}{r_1}\left(1+\frac{\lambda^2\epsilon^2}{6}\right)+\left(\frac{r_2}{r_1}-r_1\right)\theta_0\epsilon & & & \\ \frac{\mu_1}{r_1}\lambda^2\epsilon^2+2\left(\frac{r_2}{r_1}-r_1\right)\theta_1\epsilon & \frac{\mu_1}{r_1}\left(1+\frac{\lambda^2\epsilon^2}{6}\right)+\left(\frac{r_2}{r_1}-r_1\right)\theta_0\epsilon & & \\ 2\frac{\mu^1}{r_1}\lambda^2\epsilon^2+2\left(\frac{r_2}{r_1}-r_1\right)\theta_2\epsilon & \frac{\mu_1}{r_1}\lambda^2\epsilon^2+2\left(\frac{r_2}{r_1}-r_1\right)\theta_1\epsilon & \frac{\mu_1}{r_1}\left(1+\frac{\lambda^2\epsilon^2}{6}\right)+\left(\frac{r_2}{r_1}-r_1\right)\theta_0\epsilon & \\ \cdot & \cdot & \cdot & \\ \cdot & \cdot & \cdot & \\ \cdot & \cdot & \cdot & \\ (m-1)\frac{\mu_1}{r_1}\lambda^2\epsilon^2+2\left(\frac{r_2}{r_1}-r_1\right)\theta_{m-1}\epsilon & (m-2)\frac{\mu_1}{r_1}\lambda^2\epsilon^2+2\left(\frac{r_2}{r_1}-r_1\right)\theta_{m-2}\epsilon & \cdot\ \cdot\ \cdot & \frac{\mu_1}{r_1}\left(1+\frac{\lambda^2\epsilon^2}{6}\right)+\left(\frac{r_2}{r_1}-r_1\right)\theta_0\epsilon \end{bmatrix} \begin{vmatrix} \beta_1 \\ \beta_2 \\ \beta_3 \\ \cdot \\ \cdot \\ \cdot \\ \beta_m \end{vmatrix} = \mu_0 \begin{vmatrix} \alpha_1 \\ \alpha_2 \\ \alpha_3 \\ \cdot \\ \cdot \\ \cdot \\ \alpha_m \end{vmatrix} \tag{32a}$$

which may be written

$$[C]|\beta|=\mu_0|\alpha| \tag{32b}$$

The square matrix $[C]$ is seen to be similar to the other square matrices in that it is triangular with all the elements in one column made up of the elements in the previous column moved down one row.

An equation in $|\beta|$ alone is obtained by substituting $|\alpha|$ from this equation into equation (30) to yield

$$\left\{\frac{1}{\mu_0}[A][C]+[B]\right\}|\beta|=[D]|\beta|=|f| \tag{33}$$

which is the basic response equation relating β (that is, z_1'') to the gust force. This equation represents a system of

linear simultaneous equations where the order of the matrix is arbitrary; that is, the equations may be written up to any desired value of $s=m\epsilon$. The solution for response can therefore be carried on as far as desired. Fortunately, the equations are of such a nature that simultaneous solution is not required. As mentioned, each of the matrices $[A]$, $[B]$, and $[C]$ is triangular with all elements 0 above the main diagonal and with all elements on the main diagonal of each matrix equal; therefore, the main diagonal elements of $[D]$ will also all have the same value and the elements above this diagonal will be 0. If each element on the main diagonal of $[D]$ is denoted by d_1 and $[D_1]$ is the matrix $[D]$ with the main diagonal elements replaced by 0's, then

$$[D]=d_1[I]+[D_1]$$

With this equation, equation (33) may be written

$$|\beta|=\frac{1}{d_1}|f|-\frac{1}{d_1}[D_1]|\beta| \tag{34}$$

Expanded, this equation has the form

$$\begin{vmatrix}\beta_1\\ \beta_2\\ \beta_3\\ \beta_4\\ \beta_5\\ \cdot\\ \cdot\\ \cdot\end{vmatrix}=\frac{1}{d_1}\begin{vmatrix}f_1\\ f_2\\ f_3\\ f_4\\ f_5\\ \cdot\\ \cdot\\ \cdot\end{vmatrix}-\frac{1}{d_1}\begin{bmatrix}0 & & & & & & \\ d_2 & 0 & & & & & \\ d_3 & d_2 & 0 & & & & \\ d_4 & d_3 & d_2 & 0 & & & \\ d_5 & d_4 & d_3 & d_2 & 0 & & \\ \cdot & \cdot & \cdot & \cdot & \cdot & \cdot & \\ \cdot & \cdot & \cdot & \cdot & \cdot & \cdot & \\ \cdot & \cdot & \cdot & \cdot & \cdot & \cdot & \end{bmatrix}\begin{vmatrix}\beta_1\\ \beta_2\\ \beta_3\\ \beta_4\\ \beta_5\\ \cdot\\ \cdot\\ \cdot\end{vmatrix} \tag{35}$$

It can be seen that a step-by-step solution for the successive values of β may now be made; that is, β_1 is solved for first, then, with β_1 established, β_2 is solved for, and so on, as far as is desired. With the value of $|\beta|$ thus established, solution for $|\alpha|$ may now be made directly from equations (32). Values of the displacements z_0 and z_1 may be obtained directly from α and β; z_1 may be obtained from equation (31); and z_0 may be obtained from this same equation with β replaced by α.

Some mention should be made with regard to the selection of the interval ϵ. A rough guide to use in selecting ϵ can be obtained by considering λ, which appears as the characteristic frequency in most response calculations. The period based on this frequency would be $T_s=\frac{2\pi}{\lambda}$. Experience has shown that an interval in the neighborhood of 1/12 of this period yields very good results (in general less than 1 percent error); accordingly, a reasonable guide in choosing ϵ would be the equation $\epsilon\approx\frac{1}{2\lambda}$. Some convenient value near that given by this equation should be satisfactory; in general, it will be found that ϵ may be 1 or greater.

The procedure thus outlined provides a rather rapid evaluation of the response due to a prescribed gust. With the response thus evaluated, the bending moment at any value of s or the complete time history of bending moment may be found by application of equations (23).

As a convenience in making calculations, a summary of the procedure developed in this section has been made and is given in appendix B. Curves of the value of the gust force, equation (27b), are also given for three different types of discrete gusts: sine gusts, sine^2 gusts, and triangular gusts.

As a final word, it should be evident that, if response values for either z_0'' or z_1'' are known, the gust causing this response can be found by suitable manipulation of equations (30) and (32). Thus, if z_0'' is known, β in equations (30b) and (32b) may be eliminated to give the equation

$$\{[A]+\mu_0[B][C]^{-1}\}|\alpha|=|f|$$

Direct substitution of z_0'' in this equation allows $|f|$ to be determined. In most practical cases the second term in equation (30b) contributes only a small amount and may be dropped with little resulting error in the gust force. The equation for $|f|$ is then simply

$$[A]|\alpha|=|f|$$

The case of continuous-sinusoidal-gust encounter.—Of primary importance in making continuous-turbulence studies is the response of the aircraft to a continuous sinusoidal gust. A reduction of the response equations to this case is therefore now made.

Where the gust is sinusoidal with frequency ω, the quantities u, z_0, and z_1 may all be taken proportional to e^{ik_s}, where $k=\frac{\omega c_0}{2V}$, and it may be shown that equations (16) and (19) reduce to (eq. (19) is chosen in place of eq. (17) purely for convenience)

$$\mu_0 z_0''=-2(z_0'+r_1 z_1')(F+iG)+\frac{u}{l}(P+iQ) \tag{36}$$

$$\frac{\mu_1}{r_1}(z_1''+\lambda^2 z_1)+2\left(\frac{r_2}{r_1}-r_1\right)z_1'(F+iG)=\mu_0 z_0'' \tag{37}$$

where $F(k)$ and $G(k)$ are the in-phase and out-of-phase oscillatory lift coefficients used in flutter work and $P(k)$ and $Q(k)$ are the similar in-phase and out-of-phase lift components on a rigid wing subjected to a sinusoidal gust (see, for example, ref. 17).

Now let the gust velocity and the motion be represented by the real parts of

$$\left.\begin{aligned}u&=Ue^{ik_s}\\ z_0&=Z_0e^{ik_s}\\ z_1&=Z_1e^{ik_s}\end{aligned}\right\} \tag{38}$$

where Z_0 and Z_1 may be complex. With these equations, equations (36) and (37) become

$$k^2\left(-\mu_0-\frac{2G}{k}+i\frac{2F}{k}\right)Z_0+k^2\left(-r_1\frac{2G}{k}+ir_1\frac{2F}{k}\right)Z_1=P+iQ \tag{39}$$

$$k^2\mu_0 Z_0+k^2\left[\frac{\mu_1}{r_1}\left(\frac{\lambda^2}{k^2}-1\right)-\left(\frac{r_2}{r_1}-r_1\right)\frac{2G}{k}+i\left(\frac{r_2}{r_1}-r_1\right)\frac{2F}{k}\right]Z_1=0 \tag{40}$$

These equations yield

$$Z_0=\frac{(R_4+iS_4)(P+iQ)}{k^2(\Delta_1+i\Delta_2)} \tag{41}$$

$$Z_1=\frac{-R_3(P+iQ)}{k^2(\Delta_1+i\Delta_2)} \tag{42}$$

where

$$\left.\begin{aligned}
R_1&=-\mu_0-\frac{2G}{k}\\
R_2&=-r_1\frac{2G}{k}\\
R_3&=\mu_0\\
R_4&=\frac{\mu_1}{r_1}\left(\frac{\lambda^2}{k^2}-1\right)-\left(\frac{r_2}{r_1}-r_1\right)\frac{2G}{k}\\
R_5&=R_4+\left(\frac{h}{d}\frac{\lambda^2}{k^2}-\frac{e}{d}\right)R_3\\
S_1&=\frac{2F}{k}\\
S_2&=r_1\frac{2F}{k}\\
S_4&=\left(\frac{r_2}{r_1}-r_1\right)\frac{2F}{k}\\
\Delta_1&=R_1R_4-S_1S_4-R_2R_3\\
\Delta_2&=R_1S_4+R_4S_1-R_3S_2
\end{aligned}\right\} \tag{43}$$

in which R_5 has been included because it appears later. With Z_0 and Z_1 established, the various response quantities of interest may be determined. Those used frequently are (1) the rigid-body component of acceleration z_0'', (2) the acceleration at the fuselage center line

$$z''(0)=z_0''+z_1''w_1(0)=z_0''-\delta z_1''$$

where δ is the absolute value of the fundamental-mode deflection at the fuselage in terms of a unit tip amplitude, and (3) the bending-moment factor $K_j=dz_0''+ez_1''+h\lambda^2z_1$, see equation (23a). In accordance with equations (38), these quantities may be written as the real parts of

$$\left.\begin{aligned}
z_0''&=-k^2Z_0e^{ikx}\\
z''(0)&=-k^2(Z_0-\delta Z_1)e^{ikx}\\
K_j&=-k^2\left[dZ_0+\left(e-h\frac{\lambda^2}{k^2}\right)Z_1\right]e^{ikx}
\end{aligned}\right\} \tag{44}$$

With the use of equations (41) and (42), these equations become

$$\left.\begin{aligned}
z_0''&=-\frac{(R_4+iS_4)(P+iQ)}{\Delta_1+i\Delta_2}e^{ikx}\\
z''(0)&=-\frac{(R_4+\delta R_3+iS_4)(P+iQ)}{\Delta_1+i\Delta_2}e^{ikx}\\
K_j&=-\frac{d(R_5+iS_4)(P+iQ)}{\Delta_1+i\Delta_2}e^{ikx}
\end{aligned}\right\} \tag{45}$$

The squares of the amplitudes follow directly from these equations and are listed below since they play a primary role in many applications

$$|z_0''|^2=\frac{(R_4^2+S_4^2)(P^2+Q^2)}{\Delta_1^2+\Delta_2^2} \tag{46}$$

$$|z''(0)|^2=\frac{[(R_4+\delta R_3)^2+S_4^2](P^2+Q^2)}{\Delta_1^2+\Delta_2^2} \tag{47}$$

$$|K_j|^2=\frac{d^2(R_5^2+S_4^2)(P^2+Q^2)}{\Delta_1^2+\Delta_2^2} \tag{48}$$

It is worthwhile at this point to mention that a good approximation exists for the quantity P^2+Q^2 which appears in all three equations. This quantity reflects the force on the airplane due directly to the sinusoidal gust and for two-dimensional incompressible flow is approximated with good accuracy by the expression (see ref. 8)

$$P^2+Q^2=\frac{1}{1+2\pi k} \tag{49}$$

Two other quantities which are used frequently in applications are now presented. These two quantities are the acceleration and bending-moment factor that apply when the airplane is considered as a rigid body, that is, when it is considered to have only the degree of freedom of vertical motion. The equation for rigid-body response can be obtained directly from equation (39) by setting $Z_1=0$. With the aid of the resulting equation it may be shown that the square of the amplitude of the rigid-body acceleration is

$$|Z_{0_r}''|^2=\frac{P^2+Q^2}{\left(\mu_0+\frac{2G}{k}\right)^2+\left(\frac{2F}{k}\right)^2} \tag{50}$$

Through use of equation (26), the rigid-body bending-moment factor may be written

$$|K_{j_r}|^2=(\mu_0-\eta_0)^2|Z_{0_r}''|^2 \tag{51}$$

As a closing remark to this section, it may be said that the computation of the response to a continuous sinusoidal gust is actually quite an easy task, the amount of work involved being very small in comparison with that involved in a discrete-gust calculation. All that is necessary is to evaluate the response quantity of interest, equations (46) to (48), through means of the coefficients given by equations (43), with k taken equal to the reduced frequency of the sinusoidal gust under consideration. Because the computation is so straightforward, no summary is given as in appendix B for the case of discrete-gust encounter.

EXAMPLE

In order to provide an illustration and give an idea of the accuracy of the present analysis, the response to a sharp-edge gust of the two-engine-airplane example considered in reference 16 was determined. The weight distribution over the semispan, the wing-chord distribution, and the fundamental bending mode are shown in figures 2, 3, and 4. The frequency and deflection of the fundamental mode were calculated by the method given in reference 18. The solution is made for a forward velocity of 210 mph and a gust velocity of 10 ft/sec.

The lift-curve slope used in reference 16 was 5.41; to be consistent, the same value was used herein. Furthermore, the unsteady-lift function used for a change in angle of attack in the example presented in reference 16 was given by the equation

$$(1-\phi)_{A=0}=1-0.361e^{-0.381s}$$

rather than by equation (9). Thus, this equation was also used herein. The gust unsteady-lift function used was that given by equation (10).

The various physical constants and the basic response and bending-moment parameters are given in table 1; the values of the unsteady-lift function and the values of the gust force are listed in table 2. The matrices [A], [B], and [C] used in the solution are given in table 3.

The solution for response is shown in figure 5 (a) where the deflection coefficients a_0 and a_1 in inches are plotted against distance traveled in half-chords. The corresponding deflection quantities for the example given in reference 16 were determined and, for comparison, are also shown in the figure. A similar comparison is made in figure 5 (b) for bending stresses at the fuselage and engine stations, stations 0 and 1 from reference 16. The agreement is seen to be good.

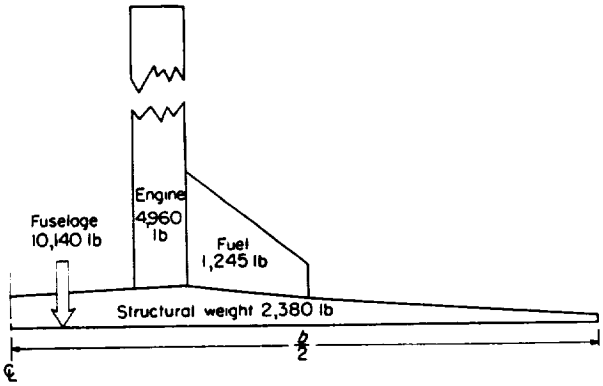

FIGURE 2.—Semispan weight distribution for the two-engine airplane of example.

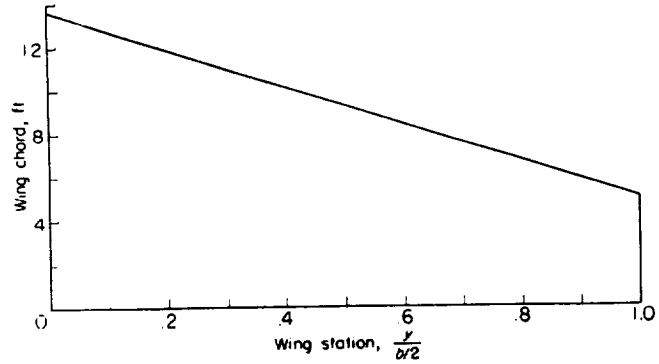

FIGURE 3.—Wing chord distribution for airplane of example.

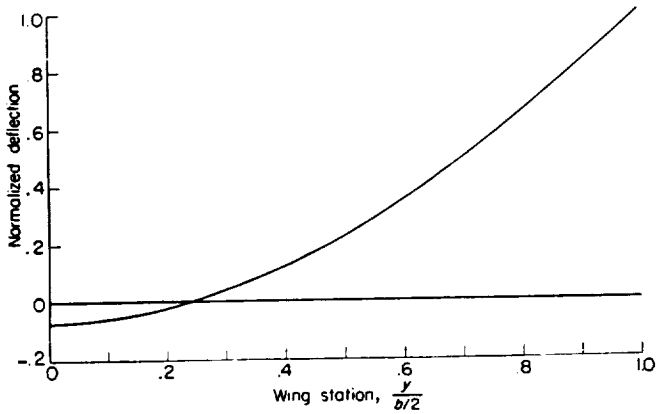

FIGURE 4.—First-symmetrical-bending-mode deflection curve of example airplane. $\omega_1=20.9$ radians/sec.

TABLE 1.—PHYSICAL CHARACTERISTICS OF AIRPLANE USED IN EXAMPLE

W, lb	37,450
S, sq ft	870
b, in.	1129
c_0, in.	154
ρ, slugs/cu ft	0.00238
V, ft/sec	308
U, ft/sec	10
s, sec	0.0208
s, half-chords	1.0
a	5.41
μ_0	64.16
μ_1	0.9045
λ	0.4353
r_1	0.2181
r_2	0.1358
r_2, fuselage station	0.452
r_2, engine station	0.547
m, fuselage station	23.49
m, engine station	10.19
m_1, fuselage station	3.665
m_1, engine station	3.391
$\frac{z}{I}$, in.$^{-2}$, fuselage station	0.00537
$\frac{z}{I}$, in.$^{-2}$, engine station	0.00669

*z here denotes distance from neutral axis to extreme fiber.

TABLE 2.— $1-\phi$ ORDINATES AND GUST-FORCE ORDINATES FOR SHARP-EDGE GUST, $\epsilon=1.0$

m	θ_m or $(1-\phi)_{A=4}$	f or ψ
0	0.6390	0
1	.7534	.377
2	.8315	.547
3	.8849	.635
4	.9214	.692
5	.9463	.736
6	.9633	.771
7	.9749	.798
8	.9829	.821
9	.9883	.845

TABLE 3.—MATRICES USED IN EXAMPLE

A Matrix

64.799										
1.5068	64.799									
1.6630	1.5068	64.799								
1.7698	1.6630	1.5068	64.799							
1.8428	1.7698	1.6630	1.5068	64.799						
1.8926	1.8428	1.7698	1.6630	1.5068	64.799					
1.9266	1.8926	1.8428	1.7698	1.6630	1.5068	64.799				
1.9498	1.9266	1.8926	1.8428	1.7698	1.6630	1.5068	64.799			
1.9658	1.9498	1.9266	1.8926	1.8428	1.7698	1.6630	1.5068	64.799		
1.9766	1.9658	1.9498	1.9266	1.8926	1.8428	1.7698	1.6630	1.5068	64.799	

B Matrix

0.1394										
.3286	0.1394									
.3627	.3286	0.1394								
.3860	.3627	.3286	0.1394							
.4019	.3860	.3627	.3286	0.1394						
.4128	.4019	.3860	.3627	.3286	0.1394					
.4202	.4128	.4019	.3860	.3627	.3286	0.1394				
.4252	.4202	.4128	.4019	.3860	.3627	.3286	0.1394			
.4287	.4252	.4202	.4128	.4019	.3860	.3627	.3286	0.1394		
.4311	.4287	.4252	.4202	.4128	.4019	.3860	.3627	.3286	0.1394	

C Matrix

4.5367										
1.3954	4.5367									
2.2445	1.3954	4.5367								
3.0735	2.2445	1.3954	4.5367							
3.8889	3.0735	2.2445	1.3954	4.5367						
4.6949	3.8889	3.0735	2.2445	1.3954	4.5367					
5.4947	4.6949	3.8889	3.0735	2.2445	1.3954	4.5367				
6.2900	5.4947	4.6949	3.8889	3.0735	2.2445	1.3954	4.5367			
7.0824	6.2900	5.4947	4.6949	3.8889	3.0735	2.2445	1.3954	4.5367		
7.8726	7.0824	6.2900	5.4947	4.6949	3.8889	3.0735	2.2445	1.3954	4.5367	

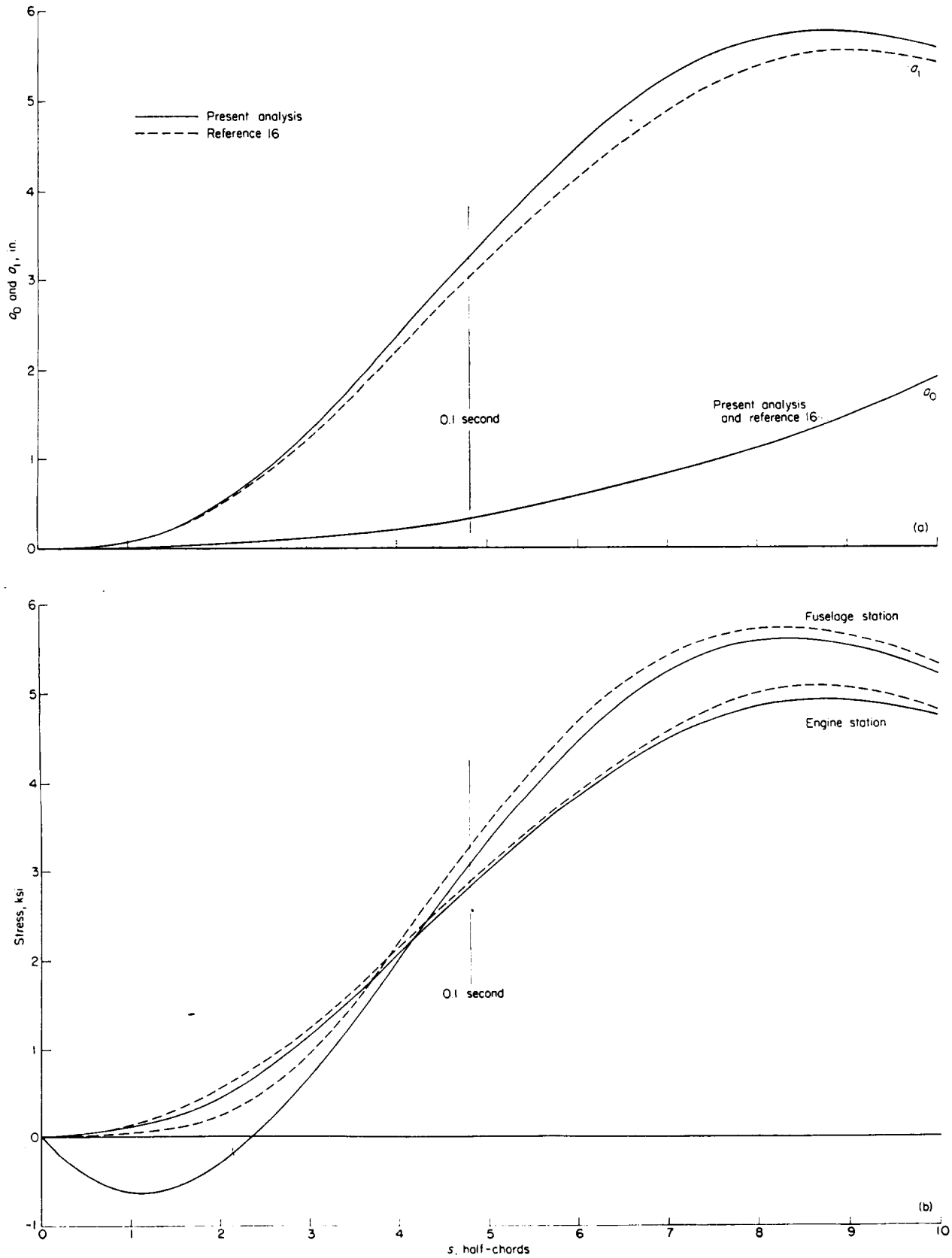

(a) Displacements.
(b) Stresses.

FIGURE 5.—Response of example airplane to a 10-ft/sec sharp-edge gust. $V=210$ mph.

REMARKS ON ANALYSIS

Although the unsteady-lift functions for two-dimensional unsteady flow are presented, the method is general enough so that the unsteady-lift functions for finite aspect ratio, for subsonic compressible flow, and for supersonic flow may be used as well. (See refs. 3 and 17 to 22.)

Since the numerical method for the case of discrete-gust encounter is based on an integration procedure, it possesses the desirable feature that a fairly large time interval may be used and good accuracy still be obtained. As an accuracy test, solutions of equations (16) and (17) were made for several cases by the exact Laplace transform method as well as by the numerical process, in which process the time interval was selected according to the rule of thumb suggested. When the results were plotted to three figures, the difference between the two solutions was barely discernible.

Additional bending modes could be included in the analysis but this refinement is really not warranted. Some calculations made with additional modes gave results which differed only slightly from the results obtained when only the fundamental mode was used. The good agreement of results obtained for the example with the results obtained by the more precise method given in reference 16 also illustrates this point. Furthermore, if additional degrees of freedom are to be used, it would appear more important to extend the analysis to include wing torsion and airplane pitch and, also, to include the case of nonuniform spanwise gusts. Torsion undoubtedly becomes important for speeds near the flutter speed, and pitch would appear important for cases where low damping in pitch is present. This latter point has been borne out by some investigations which show that there is a marked increase in gust loads as the damping in pitch is decreased. However, it is the intent of this analysis to treat the effects of wing bending flexibility and it should be sufficiently satisfactory for speeds at least up to the cruising speeds and for airplanes having good longitudinal damping characteristics.

TREATMENT OF RANDOM CONTINUOUS TURBULENCE

The approach given in the previous section works well for gusts which are either isolated or which are of a continuous-sinusoidal type. It also works for gusts which are of a random-continuous nature, such as exist in the atmosphere. For this case, however, the approach is not very practical, first because it is questionable whether an appropriate or representative time history of atmospheric gust sequence could be established, and second because for any long gust sequence the amount of computational work involved is prohibitively large. It is therefore desirable to turn to other means for treating realistic turbulence conditions, with the view of having a technique that has general applicability and is mathematically tractable.

One such procedure which suggests itself for treating the case of random continuous turbulence and which is at present receiving much attention makes use of the concepts and techniques of generalized harmonic analysis (see, for example, refs. 6 to 10). These methods permit the description of the random-atmospheric-turbulence disturbance and the associated airplane response in analytic form by means of the so-called "power-spectral-density function." A brief review of the technique is considered pertinent. If $u(t)$ represents a random disturbance or a system response quantity to this disturbance (such as the atmospheric vertical velocity and resulting structural response considered herein), then the power-spectral-density function $\Phi(\omega)$ is defined as

$$\Phi(\omega)=\lim_{T\to\infty}\frac{1}{2\pi T}\left|\int_{-T}^{T}u(t)e^{-i\omega t}dt\right|^2 \tag{52}$$

where ω is frequency in radians per second, and the bars designate the modulus of the complex quantity $\int_{-T}^{T}u(t)e^{-i\omega t}dt$, which is known as the Fourier transform of $u(t)$. An equivalent and more useful expression for $\Phi(\omega)$ can be derived and is

$$\Phi(\omega)=\frac{2}{\pi}\int_0^\infty R(\tau)\cos\omega\tau\,d\tau \tag{53}$$

where $R(\tau)$ is the autocorrelation function defined by

$$R(\tau)=\lim_{T\to\infty}\frac{1}{2T}\int_{-T}^{T}u(t)u(t+\tau)\,dt \tag{54}$$

A useful property of $\Phi(\omega)$ is that

$$\int_0^\infty\Phi(\omega)\,d\omega=\text{Mean square}=\overline{u^2(t)}=R(0)=\sigma^2 \tag{55}$$

The quantity $\overline{u^2(t)}$, or σ^2, the time mean square, provides a measure of the disturbance energy per unit time and has thus been characteristically termed the power, as a carryover from its early application in the fields of communications and turbulence, where it often had the dimensions of power. Thus, $\Phi(\omega)$ has, in turn, been termed the energy or power spectrum. In this form, the element $\Phi(\omega)\,d\omega$ gives the contribution to the mean square of harmonic components of $u(t)$ having frequencies between ω and $\omega+d\omega$.

Now a particularly useful and simple relation exists for linear systems between the spectrum of a disturbance and the spectrum of the system response to the disturbance (see refs. 8 and 23). This relation is

$$\Phi_o(\omega)=\Phi_i(\omega)\,T^2(\omega) \tag{56}$$

where

$\Phi_o(\omega)$ output spectrum
$\Phi_i(\omega)$ input spectrum
$T(\omega)$ amplitude of admittance frequency-response function which is defined as the system response to sinusoidal disturbances of various frequencies

It is precisely because of this equation that the response to a continuous sinusoidal gust was derived in the previous section. The equation indicates that the response at a given frequency depends only on the input and the system admittance at that frequency, which is plausible for linear systems.

A significant point to note here is that, despite the fact that continuous random disturbances are under consideration, the response equation (56) turns out to be surprisingly simple and easy to apply. This fortunate outcome is undoubtedly one of the consequences of working in the frequency plane rather than the time plane. Nevertheless, even though the

frequency plane is involved, it is still possible in particular cases to determine a number of statistical characteristics of the disturbance or response time histories which are of interest. For example, the root-mean-square value σ, which may be obtained directly from the spectrum in accordance with equation (55), provides a useful linear measure of the disturbance or response intensity. Further, in the particular case in which the function $u(t)$ has a normal or Gaussian probability distribution with zero mean, the probability density is given by

$$p(y)=\frac{1}{\sigma\sqrt{2\pi}}e^{-u^2/2\sigma^2} \tag{57}$$

Also, S. O. Rice, in reference 24, has derived for the case in which the disturbance function is completely Gaussian a number of relations which appear useful in aeronautical applications and which are particularly significant for fatigue studies. One of the more important expressions is for the average number of peak values (maximums) per second that are above a given value of u. For the larger values of u (say $u>2\sigma$), the expression is

$$N_p(u)=\frac{1}{2\pi}\frac{\sigma}{\sigma_1}e^{-u^2/2\sigma^2} \tag{58a}$$

where

$$\sigma_1=\left[\int_0^\infty \omega^2\Phi(\omega)\,d\omega\right]^{1/2} \tag{58b}$$

There is some indication, as described in reference 6, that airplane gust loads may tend to have a normal distribution. Hence, use is made of these equations subsequently in the application to the flexibility studies.

As a schematic illustration of the application of equation (56) to the problem of airplane response to gusts, figure 6 has been prepared. The top sketch in this figure is the input spectrum and, in this case, represents the spectrum of atmospheric vertical velocity. The frequency argument Ω, which is 2π divided by the wave length L, is introduced in place of ω because gust disturbances are essentially space disturbances rather than disturbances in time. The second sketch $T^2(\Omega)$ represents the amplitude squared of a specified airplane response, such as the airplane normal acceleration (eq. (46)) to sinusoidal gusts of unit amplitude and of frequency Ω. (Note that ω, k, and Ω are related as follows: $\omega=V\Omega=\frac{2Vk}{c_0}$.) This function introduces the characteristics of the airplane, the various modes usually showing up as peaks such as the free-body and fundamental wing-bending modes illustrated. The output spectrum $\Phi_o(\Omega)$ is obtained in accordance with equation (56) (this equation applies whether the argument is ω or Ω) as the product of the first two curves and gives, for example, the spectrum of normal acceleration or the spectrum of stress, depending upon what quantity is chosen for the frequency-response function. This output spectrum indicates the extent to which various frequency components are present in the response, and, further, it allows for the determination of various statistical properties of the response time history, such as are given by equations (55), (57), and (58).

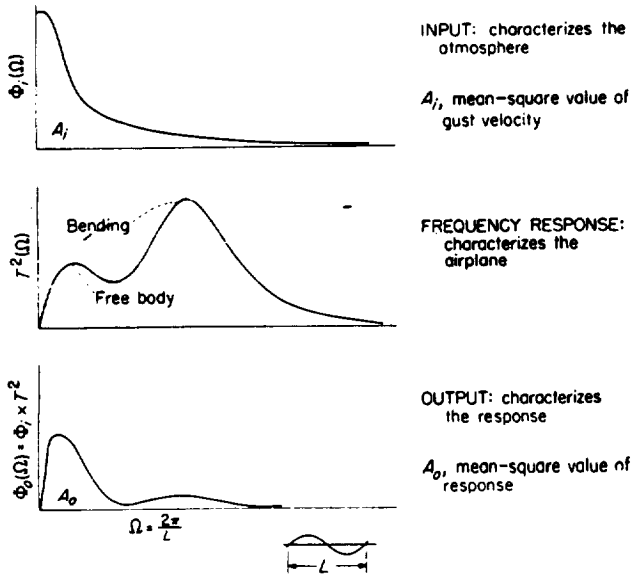

FIGURE 6.—Gust-response determination.

CORRELATION OF CALCULATION AND FLIGHT STUDIES

A number of flight and analytical studies have been made which deal with the effect of wing flexibility on the structural response of an airplane in flight through rough air (see refs. 10 to 12 and 25 to 28). The primary results of these studies are summarized in this section. Specifically, the following material is covered. The significant results of flight tests are given. Studies made on the basis of single- or discrete-gust encounter are then reviewed and the extent of the correlation with flight-test results is indicated. Finally, some analytical work on the more realistic condition of continuous-turbulence encounter is presented and correlation with flight tests shown.

FLEXIBILITY MEASURES

From an analytical point of view, several measures may be devised to indicate the extent to which flexibility effects are present in any airplane. Generally these measures indicate how a particular structural-response quantity (such as acceleration) for the flexible airplane compares with what this response would be if the aircraft behaved as a rigid body, a comparison of z_0'' with z_{0_r}'', for example. For the correlation purposes of the present report, however, the flexibility measures have been confined largely to the two types used in flight tests. One of these measures involves a comparison of the peak incremental accelerations developed at the fuselage with the peak incremental accelerations at the nodal points of the fundamental mode (see fig. 7), the latter acceleration being considered a close approximation to what the acceleration would be if the airplane were rigid. These two accelerations are of particular interest because both have been considered in the deductions of gust intensities from

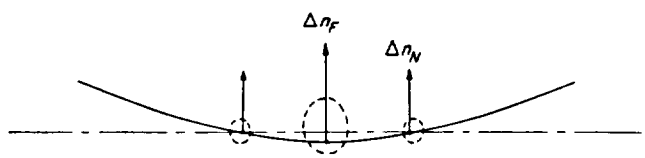

FIGURE 7.—Fuselage and nodal accelerations.

measured accelerations; they are different, in general, as are all accelerations along the wing, because of structural flexibility, particularly wing bending. The other flexibility measure involves a comparison of the actual incremental wing stresses with what these stresses would be if the airplane were rigid. Since it is, of course, not possible to obtain the rigid-body reference strains in flight, some near-equivalent strain must be used. The general practice has been to assume that the rigid-body strains are equal to the strains that would develop during pull-ups having accelerations equal to the accelerations that are measured at the nodal points during the rough-air flights, and this practice has been followed herein.

FLIGHT STUDIES

In order to establish what the numerical values of these flexibility measures are in practical cases, flight tests were made in clear rough air with the three airplanes shown in figure 8 and designated A, B, and C as shown. References 25 to 28 report some of these flight tests. These airplanes were chosen because they were available and because they were judged to be fairly representative of rather stiff, moderately flexible, and rather flexible airplanes, respectively. In this flexibility comparison, the factors which are considered to signify an increase in flexibility effects are higher operating speeds, lower natural frequencies, and greater mass in the outboard wing sections. Figure 9 shows the type of accelera-

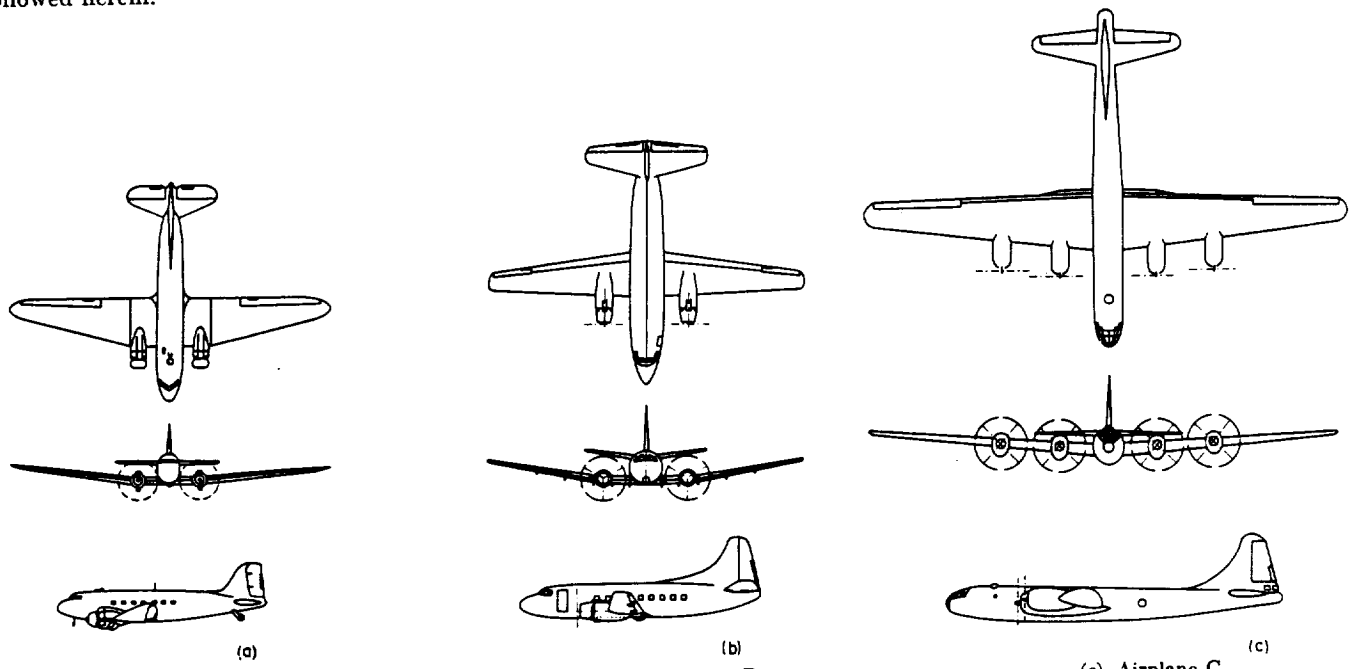

(a) Airplane A. (b) Airplane B. (c) Airplane C.

FIGURE 8.—Three-view sketches of test airplanes.

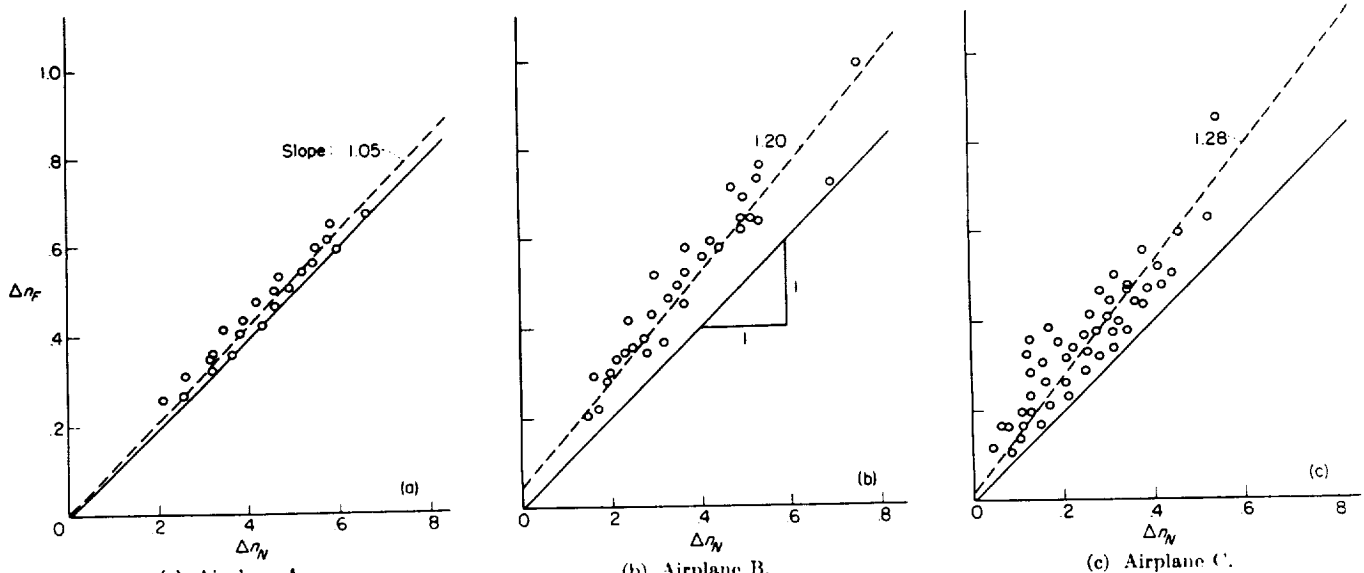

(a) Airplane A. (b) Airplane B. (c) Airplane C.

FIGURE 9.—Acceleration measured in clear rough air.

tion results obtained from these flights. The ordinate refers to peak incremental acceleration at the fuselage and the abscissa refers to the peak incremental acceleration at the nodal points. Although only positive accelerations are shown in this illustration, a similar picture was obtained for negative acceleration values. The solid line indicates a 1 to 1 correspondence; whereas the dashed line is a mean line through the flight points. The slope of this line is the amplification which results from flexibility; thus, the fuselage accelerations are 5 percent greater on the average than the nodal accelerations for airplane A, 20 percent greater for airplane B, and 28 percent greater for airplane C. It is to be remarked that the picture is not changed much if given in terms of strains; that is, if the incremental root strains for the flexible case are plotted against the strains that would be obtained if the airplane were rigid, similar amplification factors are found.

DISCRETE-GUST STUDIES

In an attempt to see whether these amplification factors could be predicted by discrete-gust studies, some calculations were made by considering the airplane to fly through single sine gusts of various lengths. The calculations were made by the discrete-gust analysis presented previously. The conditions used for speed, load distribution (payload and fuel), and total weight were similar to those used in the flight tests. Some of the significant results obtained are shown in figure 10 (see ref. 12 for additional related results). The ordinate is the ratio of the incremental root strain for the flexible airplane to the incremental root strain that is obtained for the airplane considered rigid. The abscissa is the gust-gradient distance in chords, as shown in the sketch. The curves indicate a significant increase in the amplification or response ratio in going from airplane A to B to C. It may be remarked that the amount of amplification is, in fact, related to the aerodynamic damping associated with wing-bending oscillations. This damping depends largely on the mass distribution of the airplane and is lower for higher outboard mass loadings. The curves thus reflect the successively higher outboard mass loadings of airplane B and airplane C.

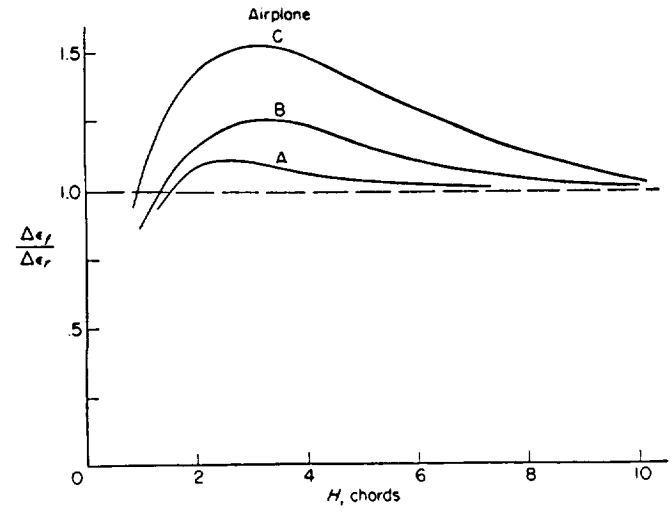

FIGURE 10.—Strain amplification for single-gust encounter.

The important point to note about this figure is that the general level of each curve is in good qualitative agreement with the amplification values found in flight. Thus, the 1.05 value for airplane A roughly represents the average of the lower curve, the 1.20 value for airplane B the average of the middle curve, and the 1.28 value for airplane C the average of the upper curve. A more direct quantitative comparison would be available if a weighted average of the calculated curves could be derived by taking into account the manner in which the gust-gradient distances are distributed in the atmosphere. No sound method is available for doing this, however, and this overall qualitative comparison will therefore have to suffice.

Figure 11 shows what is obtained when calculation and flight results are correlated in more detail. In this figure, the strain ratio is plotted against the interval of time for nodal acceleration to go from the 1 g level to a peak value. This interval, when expressed in chord lengths, is slightly different from the gust-gradient distance. The flight values shown were obtained by selecting from the continuous acceleration records a number of the more predominant humps that resembled half sine waves and then treating these humps as though they had been caused by isolated gusts. The agreement seen between the calculated results and the flight results is actually surprisingly good when the complexity of the problem and the fact that the calculations are for a highly simplified version of the actual situation are considered. In contrast to the well-behaved single gusts assumed in the calculations, the gusts encountered in flight are not isolated but are repeated and are highly irregular in shape. These factors may well account for the higher amplifications found in flight, especially in the range of higher values of time to peak acceleration; in this range it is to be expected that the amplification effects associated with the higher frequency components of the irregular gust shapes are superposed on the amplification effects of the predominant gust length to lead to the higher effective values observed.

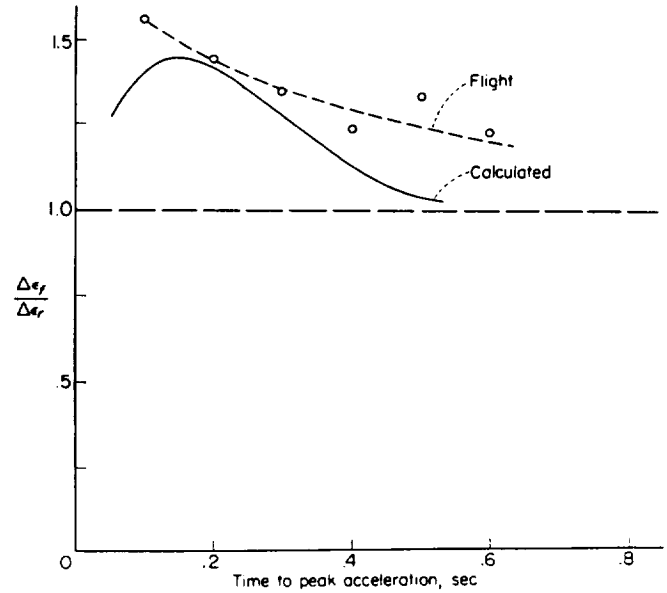

FIGURE 11.—Rough-air strain amplification for airplane C.

From the results thus far presented, it may be concluded that a reasonably fair picture of flexibility effects may be obtained with the discrete-gust approach. It is found to give good overall qualitative agreement with flight-test results and can be used to determine how one airplane compares with another in respect to the relative extent to which these effects are present. Detailed quantitative correlation is not feasible, however, since the degree of resolution permitted by the approach is limited. This is, of course, to be expected in view of the limited and unrealistic description of turbulence used.

CONTINUOUS-TURBULENCE STUDIES

The procedure given in the section entitled "Treatment of Random Continuous Turbulence" was applied in order to see what it would yield in the way of flexibility effects for the three airplanes used in the rough-air flight tests. The spectrum chosen for atmospheric vertical velocity was that given in reference 6. Bending stress at a station near the root of the wing was chosen as the response variable, and evaluation was made for flight conditions representative of those used in the flight tests. These conditions are indicated in table 4, together with the physical constants and basic parameters that apply. (It is remarked that the use of the theoretical lift-curve-slope value of 2π in place of more representative values has no serious consequence herein since the final results to be presented are in a ratio form which is relatively insensitive to the lift-curve slope used.) Figure 12 shows the transfer functions that were obtained by means of equations (48) and (51); for this evaluation the flutter coefficients for two-dimensional incompressible flow and an amplitude of the sinusoidal input gust of 1 ft/sec were used. The solid curve is for the flexible airplane and the dashed curve, for the airplane considered rigid. These curves show quite clearly the different bias that each airplane has toward various frequency components of the atmosphere. The first hump is associated with vertical translation of the airplane and the second hump, with wing bending. The spectra for bending-stress response, obtained by multiplying the frequency-response curves by the input spectrum, of course show that the curve for the flexible case overshoots the curve for the rigid case by an amount consistent with the frequency-response curves. This overshoot is a reflection in the frequency plane of the characteristics of the transient-response curves shown in figure 10. The area of the overshoot is a direct measure of the amplification in mean-square bending stress that results from wing flexibility.

TABLE 4.—AIRPLANE LOADING, PHYSICAL CONSTANTS, AND BASIC PARAMETERS

	Airplane A	Airplane B	Airplane C
Fuselage load	Crew only	$\frac{1}{2}$ full	Crew only
Fuel load	$\frac{1}{2}$ full	$\frac{1}{2}$ full	full
W, lb	24,000	33,470	105,900
V, mph	185	255	250
S, sq ft	987	870	1,739
b, in.	1,140	1,120	1,700
a	6.28	6.28	6.28
c_0, in.	170	164	205
λ	9	10	11.6
ρ, slugs/cu ft	0.00238	0.00238	0.00238
ω_1, radians/sec	27.4	21.4	15.6
μ_0	28.4	46.8	50.3
μ_1	0.266	0.748	1.132
λ_1	0.720	0.392	0.362
r_1	0.189	0.225	0.190
r_t	0.099	0.143	0.131
Wing station, in.*	50	56	60
r^2	0.375	0.457	0.417
η_0	5.56	15.94	30.88
η_1	0.918	2.56	3.63
d	7.115	4.418	1.453
e	−0.137	−0.677	−0.919
h	0.781	1.882	2.72
M_{η_0}, ft³	7,800	6,680	22,600
$\frac{z}{I}$, in.⁻³	0.00446	0.00543	0.000912

*All values listed below the wing stations apply to the station indicated.
**z here denotes distance from neutral axis to extreme fiber.

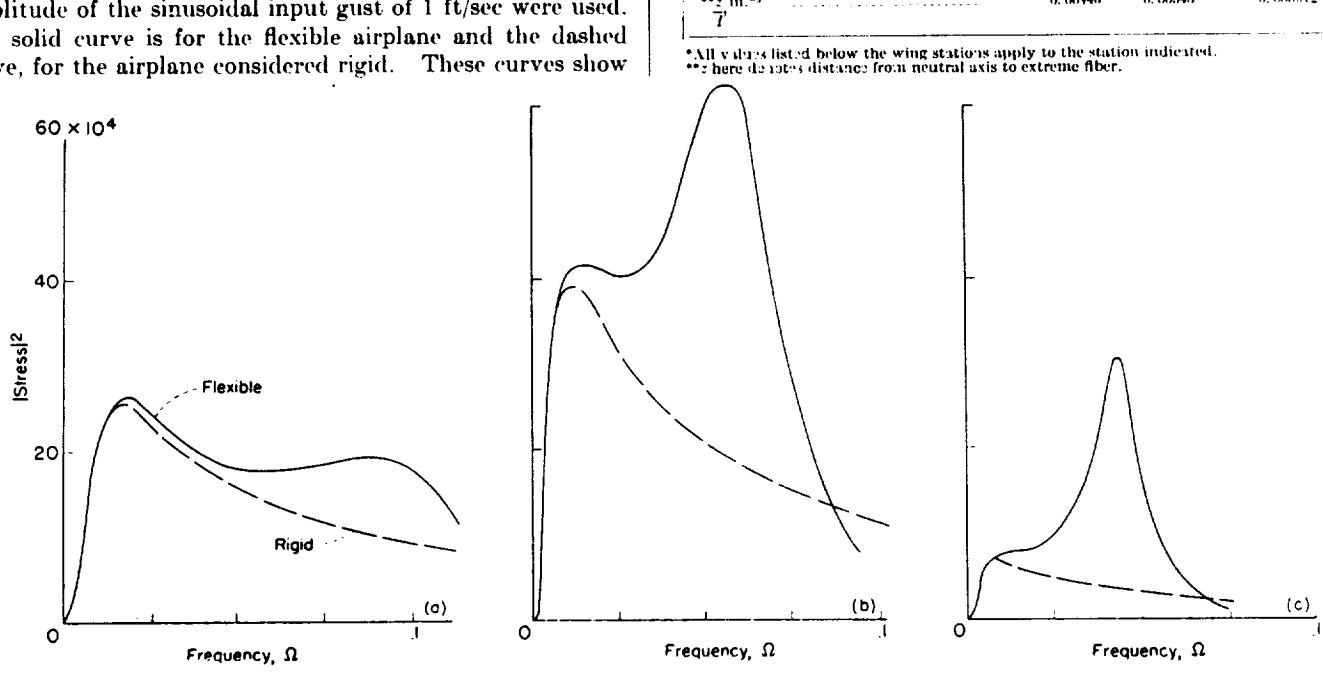

Airplane	A	B	C
Fuselage load	Crew only	$\frac{1}{2}$ full	Crew only
Fuel load	$\frac{1}{2}$ full	$\frac{1}{2}$ full	Full
Station, in.	50	56	60

(a) Airplane A. (b) Airplane B. (c) Airplane C.

FIGURE 12.—Transfer functions.

In order to obtain an amplification or flexibility measure more directly comparable to the values obtained from the flight-test results, the following procedure was used. Equations (58) were used to give curves of the type shown in sketch 1 where the ordinate N_p refers to the number of

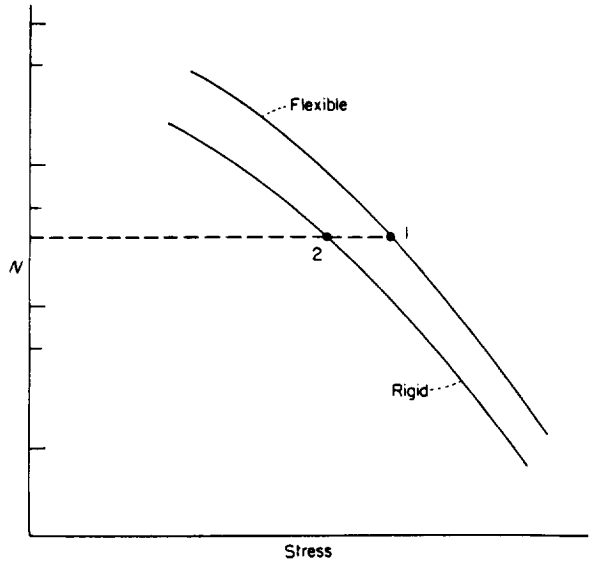

SKETCH 1.

stress peaks that occur per second above a given stress level represented by the abscissa. As can be seen, one curve applies to the flexible airplane, whereas the other is for the airplane considered rigid. A convenient measure of the magnitude of flexibility effects can be found by taking the ratio of the stress for the flexible case to the stress for the rigid case at a given value of N_p (for example, the ratio of the stress at point 1 to the stress at point 2). In general, this ratio varies with stress level; it is highest at the lower stresses and with increasing stress decreases to a constant value equal to the ratio of the root-mean-square stress for the flexible airplane to the root-mean-square stress for the rigid airplane. For correlation with flight results, this ratio was determined for each of the three airplanes. The stress level chosen was in the range of the higher flight-stress values; specifically, it was taken equal to twice the mean-square stress that developed.

Figure 13 shows a correlation of some of the results obtained by the harmonic-analysis approach with flight results. The ordinate is the previously used strain ratio, that is, the ratio of the peak incremental root bending strain for the flexible airplane to the peak incremental root bending strain for the aircraft considered rigid. The abscissa is the ratio obtained from the harmonic-analysis theory, as explained in the preceding paragraph. The three circles are the results for the three airplanes. As a matter of added interest, a single acceleration point, which was the only one computed and which applied to airplane B, has been inserted in the plot as though the coordinates involved the ratio of fuselage to nodal acceleration. The good correlation shown by this plot is, to say the least, very gratifying; it shows that good correlation may be obtained between calculations and flight results and, moreover, indicates that the harmonic-analysis approach is a suitable method to use.

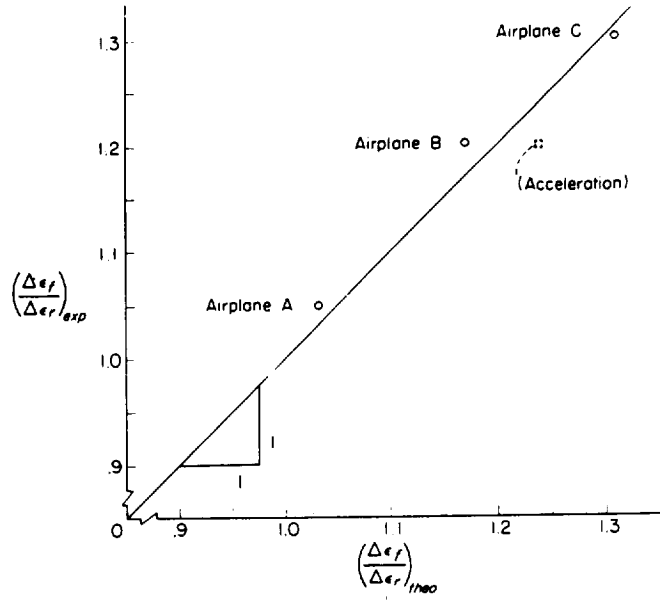

FIGURE 13.—Strain amplification for continuous turbulence.

CONCLUDING REMARKS

The derivation presented herein is intended to provide a convenient engineering method for taking into account wing bending flexibility in calculating the response of an airplane to either discrete or continuous-sinusoidal gusts. The method is believed to be well suited for making trend studies which evaluate, for example, the effect on response of such factors as mass distribution, speed, and altitude. It is not intended to apply for speeds near the flutter speed or for airplanes which have poor longitudinal damping characteristics; for these cases an extension to include wing torsion and airplane pitch would be desirable.

As regards the calculations and flight studies that were made for three airplanes to determine the manner in which gust loads are magnified by wing flexibility, the following remarks may be made. These studies indicate that an approach based upon single-gust encounter can be used to evaluate the way in which one airplane compares with another in respect to the average of these flexibility effects. This discrete-gust approach also shows overall qualitative correlation with flight results; however, it does not permit detailed resolution of the flexibility effects, and hence direct quantitative correlation is not feasible. A more appropriate approach appears to be one which considers the continuous random nature of atmospheric turbulence and which is based on generalized harmonic analysis. Not only does it permit airplanes to be compared with one another in detail but it also provides good quantitative correlation with flight results. It therefore appears that, through use of this continuous-turbulence approach, a suitable means is afforded for determining the magnitudes of flexibility effects. Moreover, many useful ramifications, such as application to fatigue studies, are provided as well.

LANGLEY AERONAUTICAL LABORATORY,
NATIONAL ADVISORY COMMITTEE FOR AERONAUTICS,
LANGLEY FIELD, VA., *March 4, 1954.*

APPENDIX A

DERIVATION OF EQUATION RELATING DISPLACEMENT TO PREVIOUS SUCCESSIVE VALUES OF ACCELERATION

In this appendix, a derivation is given of equation (31) which gives the value of displacement in terms of successive past-history values of acceleration. Suppose that the second derivative (acceleration) of a function is approximated by a succession of straight-line segments as shown in sketch 2

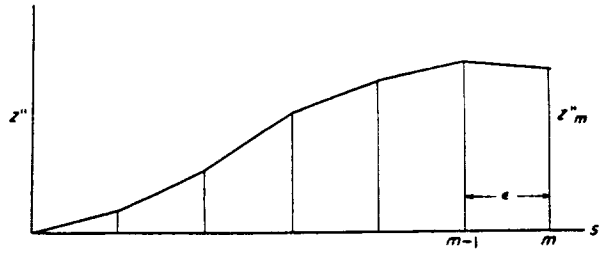

SKETCH 2.

where the segments cover equal intervals ϵ of the abscissa s and the initial condition that $z_0''=0$ is assumed to apply. If a dummy origin is now considered at the station $m-1$, the segment between stations $m-1$ and m may be represented by the equation

$$z''=z''_{m-1}+\frac{z''_m-z''_{m-1}}{\epsilon}s$$

Two successive integrations give the relations for z'_m and z_m as follows:

$$z'=z''_{m-1}s+\frac{z''_m-z''_{m-1}}{2\epsilon}s^2+z'_{m-1}$$

$$z=z''_{m-1}\frac{s^2}{2}+\frac{z''_m-z''_{m-1}}{6\epsilon}s^3+z'_{m-1}s+z_{m-1}$$

where the constants of integration z'_{m-1} and z_{m-1} (initial conditions for the interval) have been introduced. If s is set equal to ϵ in these two equations, the following equations result:

$$z'_m=\frac{\epsilon}{2}(z''_m+z''_{m-1})+z'_{m-1} \tag{A1}$$

$$z_m=\frac{\epsilon^2}{6}z''_m+\frac{\epsilon^2}{3}z''_{m-1}+z'_{m-1}\epsilon+z_{m-1} \tag{A2}$$

From these two equations the values of z'_m and z_m at any time interval may be given in terms of the second derivative at all previous time intervals. For example, with initial conditions of $z''_0=z'_0=0$, equation (A1) becomes for $m=1$

$$z'_1=\frac{\epsilon}{2}z''_1 \tag{A3}$$

and for $m=2$

$$z'_2=\frac{\epsilon}{2}(z''_2+z''_1)+z'_1$$

Combining this equation and equation (A3) results in the relation

$$z'_2=\epsilon\left(z''_1+\frac{1}{2}z''_2\right)$$

This process may be carried through for each of the time stations to yield the following general equation for z'_m:

$$z'_m=\epsilon\left(z''_1+z''_2+z''_3+\ldots+z''_{m-1}+\frac{1}{2}z''_m\right) \tag{A4}$$

which, of course, is the trapezoidal approximation of the area under the z''-curve. Equation (A2) for z_m may be treated similarly, and it is found that the general equation for z_m may be written

$$z_m=\epsilon^2\left[(m-1)z''_1+(m-2)z''_2+\ldots+2z''_{m-2}+z''_{m-1}+\frac{1}{6}z''_m\right] \tag{A5}$$

This equation thus gives the displacement at any time station in terms of the accelerations at all previous time stations.

It may be noted that, if higher-order segments (parabolic or cubic) had been used instead of straight-line segments to approximate the second derivative, equations similar in form to equations (A4) and (A5) would also result. For most practical purposes, however, the accuracy of equation (A5) is sufficiently good as long as the interval ϵ is chosen so that the straight-line segments roughly approximate the second derivative.

APPENDIX B

SUMMARY OF CALCULATION PROCEDURE FOR DETERMINING THE RESPONSE TO DISCRETE GUSTS

As a convenience, a summary of the basic steps necessary for calculating the response of an airplane to a discrete gust is given in this appendix.

For accelerations and displacements:

(1) With the use of the fundamental mode, wing plan form, and mass distribution, calculate the quantities μ_0, μ_1, λ, r_1, and r_2 as given by equations (18).

(2) Choose the time interval ϵ. A convenient rule of thumb is $\epsilon \approx \frac{1}{2\lambda}$, but for most cases $\epsilon=1$ should give satisfactory results.

(3) Determine values of the unsteady-lift function $\theta=1-\phi$ at successive multiple intervals of ϵ. (See fig. 1.) Also determine corresponding values of the gust-force integral $f(s)$, equation (27b). As an aid, curves for $f(s)$ are presented in figure 1 for the sharp-edge gust and in figure 14 for various-length sine gusts, sine^2 gusts, and triangular gusts. (The curves in fig. 1 have been obtained from eqs. (9) and (10). These approximations, although rather accurate for the lower values of s, are noted to cross; actually, they should not cross and are known to have the same asymptotic approach to unity.)

(4) From the following definitions:

$$A_1=\mu_0+\epsilon\theta_0$$

$$A_m=2\epsilon\theta_{m-1} \qquad (m>1)$$

$$B_1=r_1\epsilon\theta_0$$

$$B_m=2r_1\epsilon\theta_{m-1} \qquad (m>1)$$

$$C_1=\frac{\mu_1}{r_1}\left(1+\frac{\epsilon^2\lambda^2}{6}\right)+\left(\frac{r_2}{r_1}-r_1\right)\epsilon\theta_0$$

$$C_m=(m-1)\frac{\mu_1}{r_1}\epsilon^2\lambda^2+2\left(\frac{r_2}{r_1}-r_1\right)\epsilon\theta_{m-1} \qquad (m>1)$$

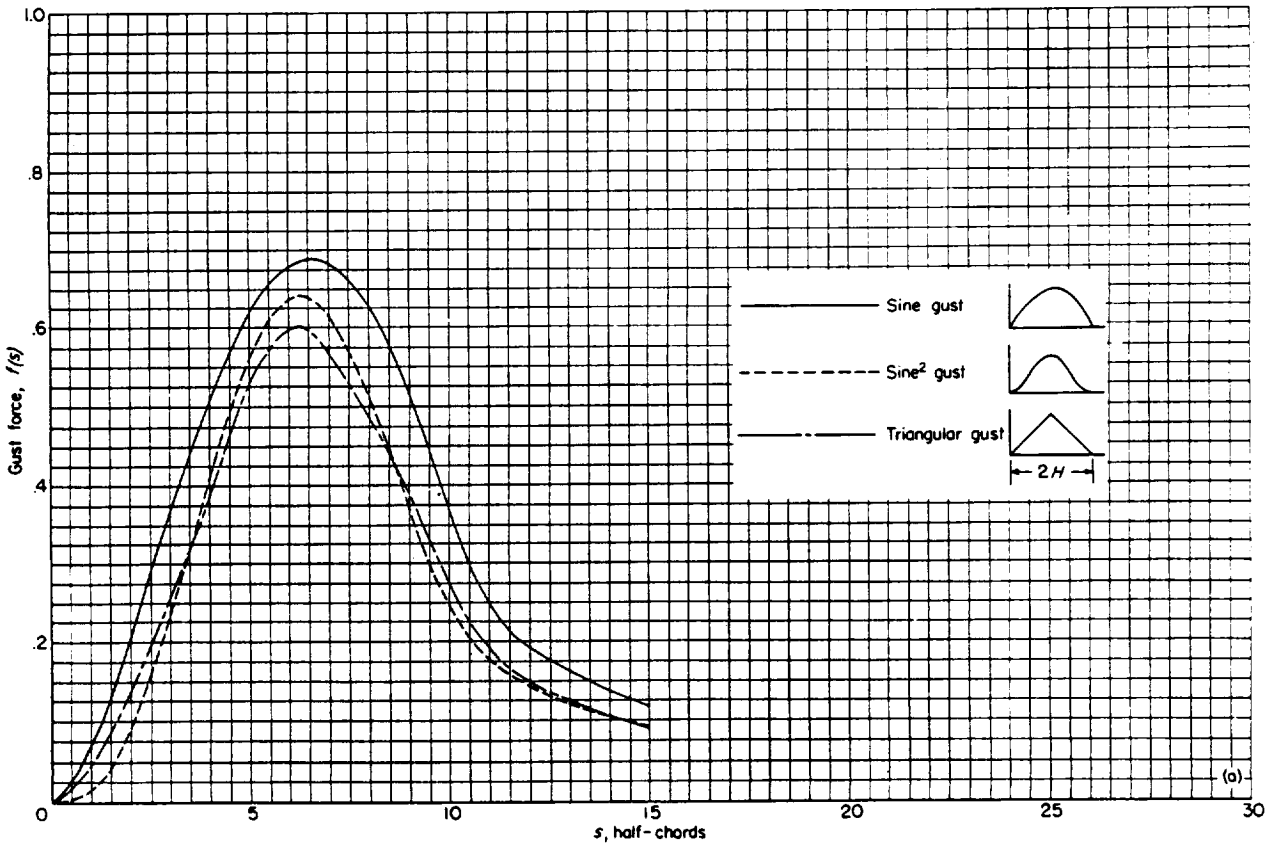

(a) $H=2.5$ chords.

FIGURE 14.—Value of the gust-force integral $f(s)=\int_0^s \frac{w'}{U}\psi(s-\sigma)d\sigma$ for three gust shapes.

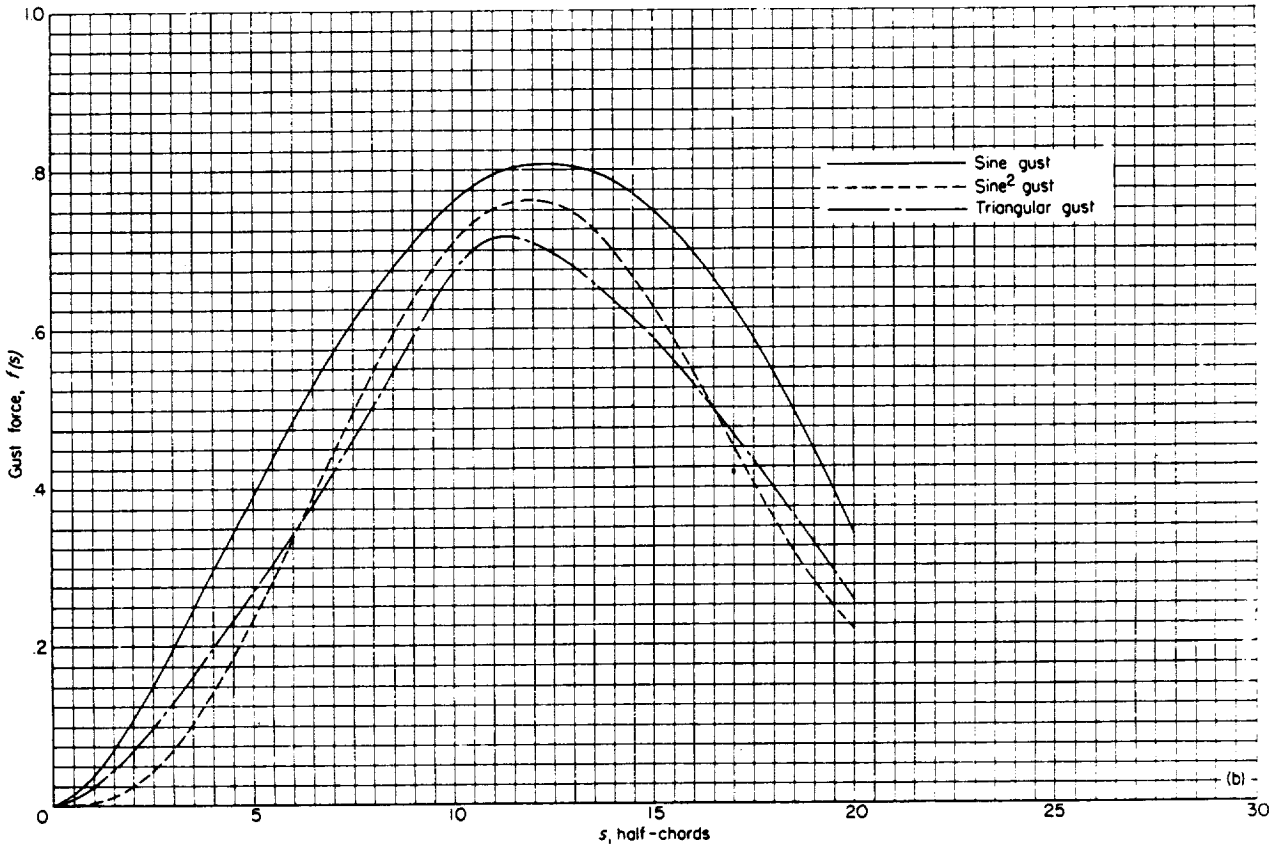

(b) $H=5$ chords.

FIGURE 14.—Continued.

set up the following matrices:

$$[A]=\begin{bmatrix} A_1 & & & & \\ A_2 & A_1 & & & \\ A_3 & A_2 & A_1 & & \\ A_4 & A_3 & A_2 & A_1 & \\ . & . & . & . & . \\ . & . & . & . & . \\ . & . & . & . & . \end{bmatrix}$$

$$[B]=\begin{bmatrix} B_1 & & & & \\ B_2 & B_1 & & & \\ B_3 & B_2 & B_1 & & \\ B_4 & B_3 & B_2 & B_1 & \\ . & . & . & . & . \\ . & . & . & . & . \\ . & . & . & . & . \end{bmatrix}$$

$$[C]=\begin{bmatrix} C_1 & & & & \\ C_2 & C_1 & & & \\ C_3 & C_2 & C_1 & & \\ C_4 & C_3 & C_2 & C_1 & \\ . & . & . & . & . \\ . & . & . & . & . \\ . & . & . & . & . \end{bmatrix}$$

Then, calculate the matrix

$$[D]=\frac{1}{\mu_0}[A][C]+[B]$$

(5) Solve for the values of β (which equals z_1'') from equation (33) by the method outlined after equation (33). (See eq. (34).) The values of z_1 and α (which equals z_0'') can then be calculated from equations (31) and (32).

For bending moment:

(6) In order to compute bending moment, determine r_3, η_0, and η_1 as given by equations (24), where M_{m_0}, M_{m_1}, M_{c_0},

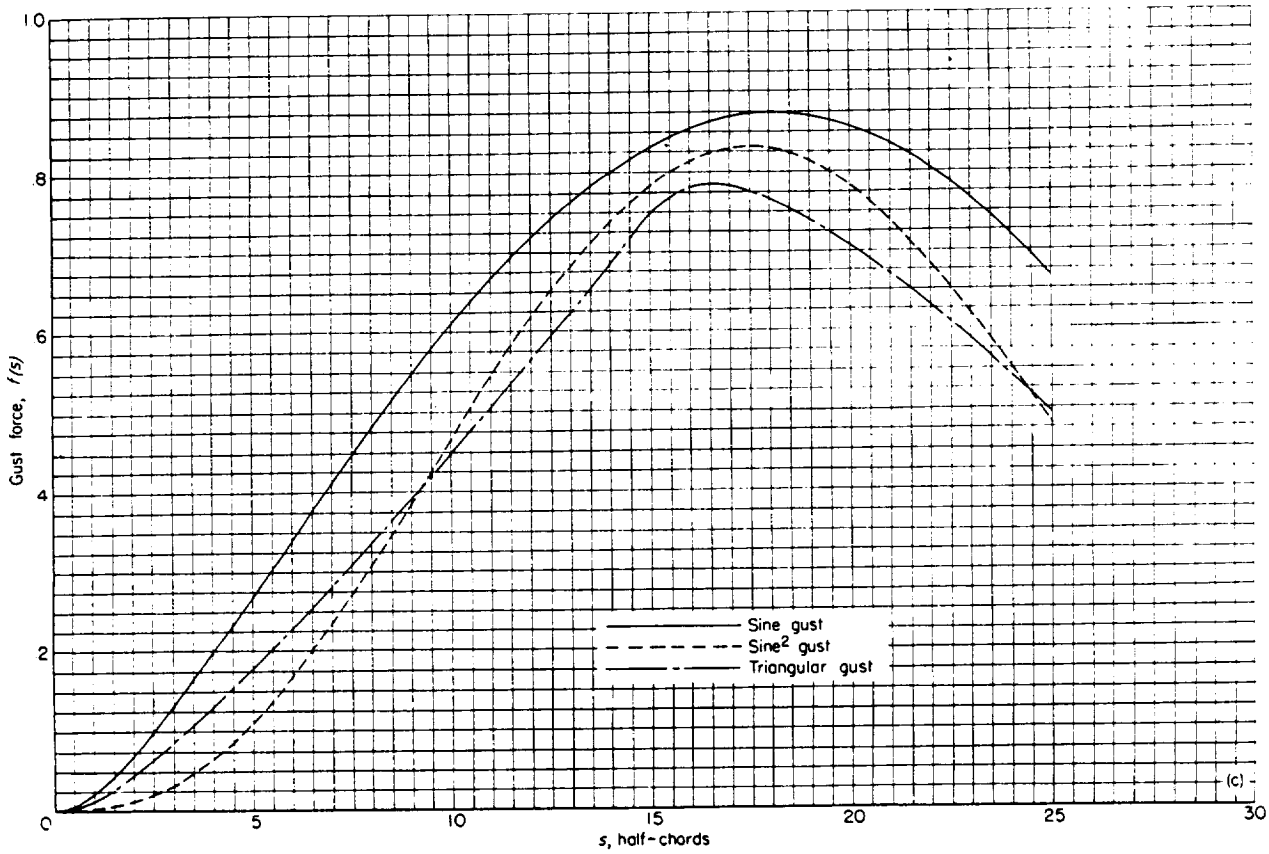

(c) $H = 7.5$ chords.

FIGURE 14.—Continued.

and M_{c_1} in these equations depend on the particular wing station being considered and are given by equations (21).

(7) Determine bending moment by use of equations (23) with the values of response already established. This equation may be applied directly to any desired time value. Maximum bending moment usually occurs very close to the time when z_1 is a maximum.

REFERENCES

1. Donely, Philip: Summary of Information Relating to Gust Loads on Airplanes. NACA Rep. 997, 1950. (Supersedes NACA TN 1976.)
2. Bisplinghoff, R. L., Isakson, G., and O'Brien, T. F.: Gust Loads on Rigid Airplanes With Pitching Neglected. Jour. Aero. Sci., vol. 18, no. 1, Jan. 1951, pp. 33–42.
3. Bisplinghoff, R. L., Isakson, G., and O'Brien, T. F.: Report on Gust Loads on Rigid and Elastic Airplanes. Contract No. NOa(s) 8790, M.I.T. Rep., Bur. Aero., Aug. 15, 1949. (This citation is intended to include ref. 3 of this reference paper which is listed therein as "Greidanus, J. H.: 'The Loading of Airplane Structures by Symmetrical Gusts' (in Dutch with an English summary). Nationaal Luchtvaartlaboratorium, Amsterdam, Rapport No. XIV, 1948.")
4. Mazelsky, Bernard: Charts of Airplane Acceleration Ratio for Gusts of Arbitrary Shape. NACA TN 2036, 1950.
5. Greidanus, J. H., and Van de Vooren, A. I.: Gust Load Coefficients for Wing and Tail Surfaces of an Aeroplane. Rep. F.28, Nationaal Luchtvaartlaboratorium, Amsterdam, Dec. 1948.
6. Press, Harry, and Mazelsky, Bernard: A Study of the Application of Power-Spectral Methods of Generalized Harmonic Analysis to Gust Loads on Airplanes. NACA TN 2853, 1953.
7. Clementson, Gerhardt C.: An Investigation of the Power Spectral Density of Atmospheric Turbulence. Ph.D. Thesis, M.I.T., 1950.
8. Liepmann, H. W.: On the Application of Statistical Concepts to the Buffeting Problem. Jour. Aero. Sci., vol. 19, no. 12, Dec. 1952, pp. 793–800, 822.
9. Fung, Y. C.: Statistical Aspects of Dynamic Loads. Jour. Aero. Sci., vol. 20, no. 5, May 1953, pp. 317–330.
10. Houbolt, John C.: Correlation of Calculation and Flight Studies of the Effect of Wing Flexibility on Structural Response Due to Gusts. NACA TN 3006, 1953.
11. Houbolt, John C., and Kordes, Eldon E.: Gust-Response Analysis of an Airplane Including Wing Bending Flexibility. NACA TN 2763, 1952.
12. Kordes, Eldon E., and Houbolt, John C.: Evaluation of Gust Response Characteristics of Some Existing Aircraft With Wing Bending Flexibility Included. NACA TN 2897, 1953.
13. Bisplinghoff, R. L., Isakson, G., Pian, T. H. H., Flomenhoft, H. I., and O'Brien, T. F.: An Investigation of Stresses in Aircraft Structures Under Dynamic Loading. Contract No. NOa(s) 8790, M. I. T. Rep., Bur. Aero., Jan. 21, 1949.

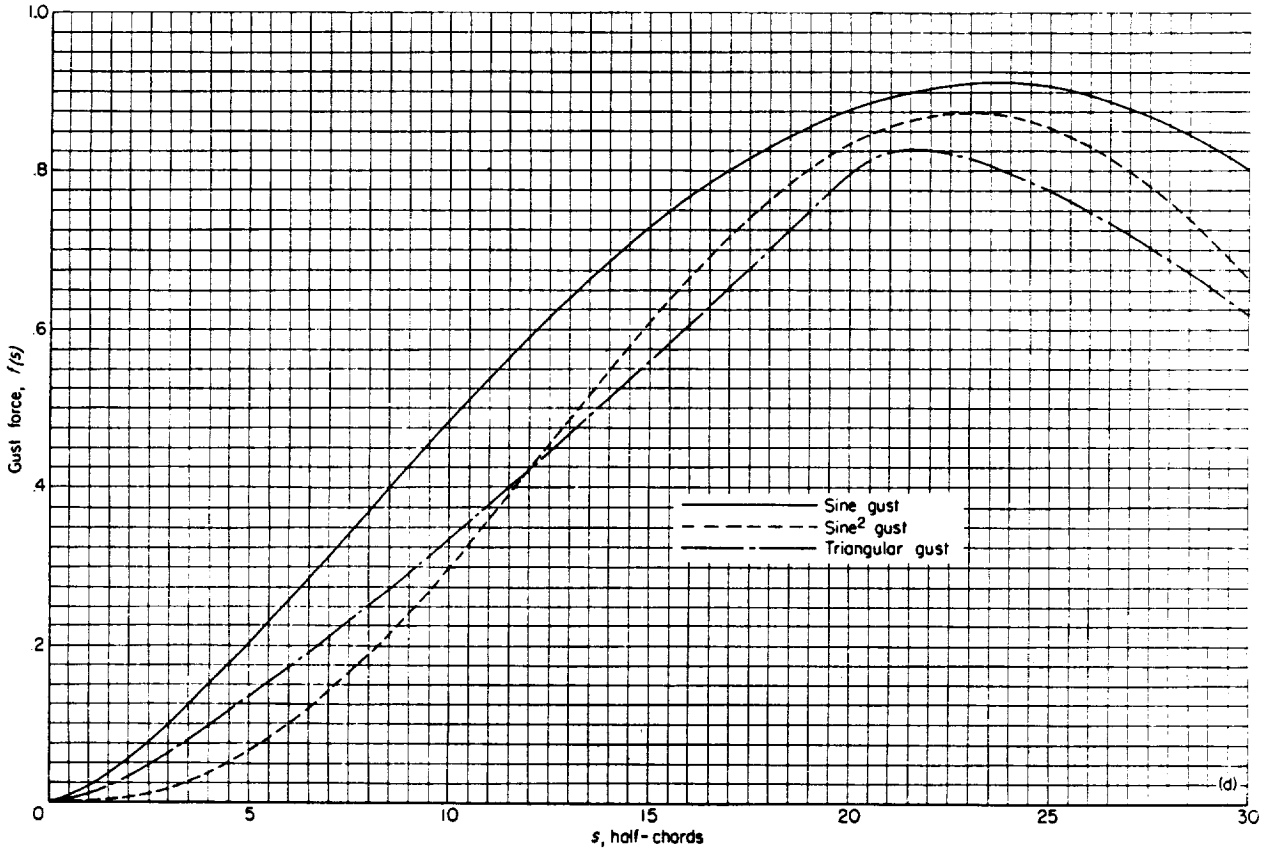

(d) $H=10$ chords.

FIGURE 14.—Concluded.

14. Goland, M., Luke, Y. L., and Kahn, E. A.: Prediction of Wing Loads Due to Gusts Including Aero-Elastic Effects. Part I—Formulation of the Method. AF TR No. 5706, Air Materiel Command, U. S. Air Force, July 21, 1947.
15. Radok, J. R. M., and Stiles, Lurline F.: The Motion and Deformation of Aircraft in Uniform and Non-Uniform Atmospheric Disturbances. Rep. ACA-41, Council for Sci. and Ind. Res., Div. Aero., Commonwealth of Australia, 1948.
16. Houbolt, John C.: A Recurrence Matrix Solution for the Dynamic Response of Aircraft in Gusts. NACA Rep. 1010, 1951. (Supersedes NACA TN 2060.)
17. Jones, Robert T.: The Unsteady Lift of a Wing of Finite Aspect Ratio. NACA Rep. 681, 1940.
18. Houbolt, John C., and Anderson, Roger A.: Calculation of Uncoupled Modes and Frequencies in Bending or Torsion of Nonuniform Beams. NACA TN 1522, 1948.
19. Radok, J. R. M.: The Problem of Gust Loads on Aircraft. A Survey of the Theoretical Treatment. Rep. SM. 133, Dept. Supply and Dev., Div. Aero., Commonwealth of Australia, July 1949.
20. Biot, M. A.: Loads on a Supersonic Wing Striking a Sharp-Edged Gust. Jour. Aero. Sci., vol. 16, no. 5, May 1949, pp. 296–300, 310.
21. Miles, John W.: Transient Loading of Supersonic Rectangular Airfoils. Jour. Aero. Sci., vol. 17, no. 10, Oct. 1950, pp. 647–652.
22. Miles, John W.: The Indicial Admittance of a Supersonic Rectangular Airfoil. NAVORD Rep. 1171, U. S. Naval Ord. Test Station (Inyokern, Calif.), July 21, 1949.
23. James, Hubert M., Nichols, Nathaniel B., and Phillips, Ralph S.: Theory of Servomechanisms. McGraw-Hill Book Co., Inc., 1947, pp. 262–307.
24. Rice, S. O.: Mathematical Analysis of Random Noise. Pts. I and II. Bell Syst. Tech. Jour., vol. XXIII, no. 3, July 1944, pp. 282–332; Pts. III and IV, vol. XXIV, no. 1, Jan. 1945, pp. 46–156.
25. Shufflebarger, C. C., and Mickleboro, Harry C.: Flight Investigation of the Effect of Transient Wing Response on Measured Accelerations of a Modern Transport Airplane in Rough Air. NACA TN 2150, 1950.
26. Mickleboro, Harry C., and Shufflebarger, C. C.: Flight Investigation of the Effect of Transient Wing Response on Wing Strains of a Twin-Engine Transport Airplane in Rough Air. NACA TN 2424, 1951.
27. Mickleboro, Harry C., Fahrer, Richard B., and Shufflebarger, C. C.: Flight Investigation of Transient Wing Response on a Four-Engine Bomber Airplane in Rough Air With Respect to Center-of-Gravity Accelerations. NACA TN 2780, 1952.
28. Murrow, Harold N., and Payne, Chester B.: Flight Investigation of the Effect of Transient Wing Response on Wing Strains of a Four-Engine Bomber Airplane in Rough Air. NACA TN 2951, 1953.

U. S. GOVERNMENT PRINTING OFFICE 1955